Strål
säkerhets
myndigheten
Swedish Radiation Safety Authority

Authors: Stuart Stothoff
Chandrika Manepally

Technical Note

2013:36

Review and assessment of aspects of the Qeq concept

Main Review Phase

Report number: 2013:36 **ISSN:** 2000-0456
Available at www.stralsakerhetsmyndigheten.se

SSM perspektiv

Bakgrund

Strålsäkerhetsmyndigheten (SSM) granskar Svensk Kärnbränslehantering AB:s (SKB) ansökningar enligt lagen (1984:3) om kärnteknisk verksamhet om uppförande, innehav och drift av ett slutförvar för använt kärnbränsle och av en inkapslingsanläggning. Som en del i granskningen ger SSM konsulter uppdrag för att inhämta information och göra expertbedömningar i avgränsade frågor. I SSM:s Technical note-serie rapporteras resultaten från dessa konsultuppdrag.

Projektets syfte

Det övergripande syftet med projektet är att ta fram synpunkter på SKB:s säkerhetsanalys SR-Site för den långsiktiga strålsäkerheten hos det planerade slutförvaret i Forsmark. Det specifika syftet med detta granskningsuppdrag är att utvärdera de modeller och angreppssätt som SKB har utvecklat för att beskriva diffusiv transport av lösta ämnen i det tilltänkta slutförvarets närområde. Detta angreppssätt benämns Qeq konceptet och tillämpas i SKB:s beräkningar av kapselkorrosion och i SKB:s beräkningar av radionuklidtransport från en skadad kapsel till geosfären.

Författarnas sammanfattning

Det tekniska granskningsuppdraget som redovisas i denna rapport utgår från de modeller och angreppssätt som SKB har utvecklat för att beskriva transport av lösta ämnen i det tilltänkta slutförvarets närområde på Forsmarksplatsen. Närmare bestämt granskas Qeq konceptet för diffusiv transport. SKB tillämpar Qeq parametern för att skala koncentrationsgradienter med målet att uppskatta lösta ämnens flux från fjärrområdet till kapselytan eller från en skadad kapsel till fjärrområdet. För att genomföra uppdraget har vi (i) granskat relevanta SKB rapporter som tillämpar Qeq konceptet, (ii) sammanfattat SKB:s tillvägagångssätt och kontrollerat överensstämmelsen av beskrivningar och valet av parametrar, (iii) identifierat risksignifikanta aspekter i angreppssättet, (iv) jämfört SKB:s beräkningar och tillvägagångssätt med oberoende beräkningar, vilket innefattar oberoende numerisk modellering och (v) genomfört en oberoende bedömning av ett värsta tänkbara scenario kopplat till Qeq konceptet.

Vi anser att Qeq konceptet som SKB har tillämpat är en rimlig och gångbar numerisk ansats för att beräkna transporten av korrodanter och radionuklider i ett slutförvars närområde. Angreppssättet tillämpas i övrigt i ett antal av matematiska fysikens grenar. Metoden som tillämpas för att beräkna resistanser är baserad på analytiska ansatser. Våra oberoende detaljerade numeriska beräkningar gav resultat som är i överensstämmelse med Qeq konceptets resultat. Qeq ansatsen är mest noggrann för icke-sorberande eller svagt sorberande lösta ämnen, vilket (i) överensstämmer med egenskaperna av de ämnena som är av intresse för korrosion och (ii) typiskt sett motsvarar egenskaperna av de radionuklider som ger de största dosbidragen. Således drar vi slutsatsen att metoden presterar bäst för de mest risksignifikanta lösta ämnena. Vissa antagenden för transportberäkningarna beskriver SKB på ett icke-konsistent sätt i deras utsläppsmodell.

Vi uppskattar att en felaktig tillämpning skulle kunna överskatta utsläppsrater med upp till en faktor tre.

Qeq ansatsen är väl lämpad för att identifiera risksignifikanta begränsningar av transporten av lösta ämnen. Beroende på scenariot kan följande punkter inverka på begränsningen av kapselkorrosionen (i) flödet i det omgivande spricksystemet, (ii) diffusion i bufferten, (iii) aspekter av systemet som förstärker konvergens av flöde till deponeringshålet och (iv) advektion (eller avsaknad därav) i deponeringshålet. Samma potentiella begränsningar föreligger för utsläppsraterna av radionuklider. I detta fall tillkommer dock begränsningar för radionuklidtransporten genom kapselhöljet, skadezoner i berget och tillfartstunnlarna.

Vi anser att beräkningarna av kapselbrott till följd av korrosion är mer risksignifikanta än radionuklidtransportberäkningarna eftersom det är högst osannolikt att ett kapselbrott inträffar i det av SKB beskrivna korrosionsscenariot. Våra oberoende beräkningar av sulfidinducerad korrosion är i överensstämmelse med SKB:s beräkningar. Vi utvecklade en alternativ konceptuell modell för uppskattning av de värsta tänkbara kopparkorrosionsraterna. Denna modell inspirerades av kanalbildningen som har observerats i laboratorieexperiment som har undersökt bentonitåtermättnad. Under antagandet att kanaler som tangerar kapselytan skulle förväntas formas i deponeringshålen med de högsta flödena (vilket vi anser är ett stort antagande), uppskattar vi att storleksordningen 0,5 procent av kapslarna möjligtvis skulle kunna korrodera igenom inom en miljon år. Genom att tillämpa jämförelsebara utsläppsberäkningar som SKB har utfört på detta värsta tänkbara fall uppskattar vi att de förväntade doserna skulle kunna närma sig riskgränsen som ges i SSM:s föreskrifter.

Projektinformation
Kontaktperson på SSM: Georg Lindgren
Diarienummer ramavtal: SSM2011-3639
Diarienummer avrop: SSM2013-2408
Aktivitetsnummer: 3030012-4054

SSM perspective

Background

The Swedish Radiation Safety Authority (SSM) reviews the Swedish Nuclear Fuel Company's (SKB) applications under the Act on Nuclear Activities (SFS 1984:3) for the construction and operation of a repository for spent nuclear fuel and for an encapsulation facility. As part of the review, SSM commissions consultants to carry out work in order to obtain information and provide expert opinion on specific issues. The results from the consultants' tasks are reported in SSM's Technical Note series.

Objectives of the project

The general objective of the project is to provide review comments on SKB's postclosure safety analysis, SR-Site, for the proposed repository at Forsmark. The specific objective of this review assignment is to evaluate the models and approaches that SKB has developed to describe diffusive transport of solutes in the nearfield of the planned repository. This approach is named the Qeq concept and applied in SKB's calculations of copper corrosion and SKB's calculations of radionuclide transport from a breached canister to the geosphere.

Summary by the authors

This technical review assignment considers the models and abstractions that Swedish Nuclear Fuel and Waste Management Company (SKB) developed to represent transport of dissolved constituents in the near field at the Forsmark site, in particular the Qeq abstraction for diffusive transport. SKB uses the Qeq parameter to scale concentration gradients in order to estimate dissolved-species fluxes from the far-field environment to the canister surface and from a canister breach to the far field. To accomplish the review assignment, we (i) reviewed relevant SKB reports that used the Qeq approach; (ii) summarized SKB's approaches, checking for consistency in the descriptions and parameter choices; (iii) identified risk-significant aspects of the approach; (iv) compared SKB calculations and approaches to independent calculations, including independent numerical modelling; (v) and independently assessed a worst-case corrosion scenario linked to the Qeq approach.

We consider the Qeq approach implemented by SKB to be a reasonable and practical numerical method, widely applied across a variety of branches of mathematical physics, for approaching the transport of corrodants and radionuclides within the near field. The methods for calculating resistances are based on analytical approaches. Our independent calculations using detailed numerical models provided results consistent with the Qeq approach. The Qeq approach is most accurate for nonsorbing or weakly sorbing dissolved species, which (i) describes the species of interest for corrosion and (ii) typically provide the largest contributions to dose. Therefore, we conclude that the method performs best on the most risk-significant dissolved constituents. SKB inconsistently describes transport assumptions in the release model; we estimate that an incorrect implementation would overestimate release rates by up to a factor of three.

The Qeq approach is well suited for identifying risk-significant constraints. Depending on the scenario, constraints on copper overpack corrosion rates include (i) flow in the surrounding fracture system, (ii) buffer diffusion, (iii) aspects of the system augmenting flow convergence to the deposition hole, and (iv) advection (or lack thereof) within the deposition hole. The same potential constraints exist for release rates, adding the constraints of transport through the canister wall, excavation damaged zone, and access tunnel.

We consider corrosion failure calculations to be risk-significant compared to radionuclide transport calculations for this site, because it is highly unlikely that a canister will fail under the nominal scenario. Our independent calculations for sulphide-induced corrosion are consistent with SKB calculations. We developed an alternative conceptual model for estimating worst-case corrosion failure rates, inspired by piping observed in laboratory experiments of bentonite rewetting. Assuming that pipes that contact the canisters would be expected to form for the deposition holes with highest flow rates (which we consider a big assumption), we estimate that on the order of 0.5 percent of the canisters might fail within one million years. Applying comparable SKB release calculations to this worst-case scenario, we estimate that expected doses might approach the regulatory limit.

Project information
Contact person at SSM: Georg Lindgren

Strål
säkerhets
myndigheten
Swedish Radiation Safety Authority

Authors: Stuart Stothoff and Chandrika Manepally
Southwest Research Institute®, San Antonio, TX, USA

Technical Note 44

2013:36

Review and assessment of aspects of the Qeq concept

Main Review Phase

Date: December 2013
Report number: 2013:36 **ISSN:** 2000-0456
Available at www.stralsakerhetsmyndigheten.se

This report was commissioned by the Swedish Radiation Safety Authority (SSM). The conclusions and viewpoints presented in the report are those of the author(s) and do not necessarily coincide with those of SSM.

Contents

1. Introduction

Flow and transport processes occur at the Forsmark site over a wide range of scales, ranging from the hundreds of meters vertical separation between the repository and ground surface to flow and transport processes occurring in individual fractures that have apertures on the order of 10 to 100 μm. Swedish Nuclear Fuel and Waste Management Company (SKB) uses nested models that embed smaller scale models into larger scale models to maintain the necessary detail at each scale. At the repository scale, before radionuclides enter into the fractures in the bed rock, diffusion processes dominate the transport. This review document focuses on near-field transport modelling.

SKB considers transport of dissolved species within the near field and engineered barrier system in two contexts: (i) corrosion of the copper overpack by reactive species from the natural environment, and (ii) release of radionuclides from a failed package. For performance assessment calculations, SKB describes the rate of transport through the engineered barrier system as a diffusive process between the far field and a degrading surface (i.e., the canister or the degrading fuel). The SKB approach combines the resistance to diffusion across a series of diffusion legs into a single effective diffusion coefficient that is used to estimate an equivalent flow rate that SKB calls Qeq (m^3/year). The Qeq parameter accounts for variable diffusion geometries within each leg. The innermost leg of the diffusion chain is at the corrosion surface. The outermost leg of the diffusion chain consists of an advection boundary, with the diffusion parameter in the outermost leg determined by the transit time of the fluid as it receives the diffusing solute. SKB uses different flow and transport models within the near field and far field, linked with common water velocities and dissolved-species fluxes at the advection boundary. The SKB considers a time scale of one million years after closure for the safety assessment and a time scale of one hundred thousand years for quantitative risk analyses.

The SKB safety case recognizes that corrosion of a copper surface proceeds very slowly, limited by the rate that the natural environment can supply adverse species, such as sulphide or oxygen, through the sparse fracture network and thick bentonite buffer. Under nominal conditions, SKB calculates that the 5 cm copper shell on each canister will take at least tens of millions of years to fail by general corrosion processes. SKB considered adverse conditions that would either degrade the buffer or induce a breach in the canister through some mechanism other than general corrosion. SKB considers canister penetration mechanisms to have such low probability of occurrence that it is unlikely that a waste package will be breached during the performance period and highly unlikely that more than one or two packages will be breached, even when natural variability is considered. Of the unlikely processes, SKB considers consequences that might arise from (i) an initial manufacturing failure (a pinhole), (ii) isostatic pressures during glaciations, and (iii) large-scale erosion of the bentonite buffer stemming from an undetected high-flow fracture intersecting the deposition hole in combination with adverse geochemical conditions penetrating to the repository depth. In the eroded buffer scenario, SKB performs calculations to estimate the time that the buffer might fail, but limits corrosion and subsequent release calculations to a scenario describing the eroded buffer configuration that SKB describes as pessimistic.

This technical review assignment considers the models and abstractions that SKB developed to represent transport of dissolved constituents in the near field, in

particular the Qeq abstraction for diffusive transport. The Qeq parameter scales concentration gradients to estimate dissolved-species fluxes from the far-field environment to the canister surface and from a canister breach to the far field. The review focuses on key controls (such as the number of failed canisters) and minimally considers processes such as sorption or radioactive decay. Because SKB assigns a low probability that any canister will be breached during the performance period, the number of waste packages that are breached is a key control on release rates, thus the technical review also considered alternative conceptual models for transport of adverse chemical species from the environment to the canister surface.

2. Assessment of the SKB Qeq model

Our assessment of the SKB Qeq model consists of two broad components, a summary of the approaches used by SKB (Section 2.1) and a technical assessment of selected risk-significant aspects of near-field transport related to Qeq (Section 2.3).

2.1. SKB's presentation

SKB considers near-field transport in the context of both copper shell corrosion and radionuclide release. We examined a variety of SKB documents, including the license application (TR-11-01), model reports, and data reports, to assess how the Qeq model is used and supported in the SKB safety analysis. After checking for consistency between documents, we focused on three reports (TR-10-42, TR-10-50, and TR-10-66) that most directly use and describe the Qeq concept. In Section 2.1, we describe SKB's presentation of the Qeq concept and implementation without offering our interpretation; the description is to be understood as representing SKB's presentation. Our intention in Section 2.1 is to collect aspects of the approach scattered across several documents into a single reference location.

2.1.1. Relationship of Qeq to Safety Functions

The ability of the host rock to provide favourable hydrogeologic and transport conditions (Safety Function R2) is influenced by the flow rate at the buffer/host rock interface (Qeq) (TR-11-01, Section 8.3.4). The amount of flow into the buffer is dependent on (i) diffusive conditions in the buffer, (ii) limited flow in the rock fractures intersecting the deposition hole, and (iii) a limited intersection area over which the exchange of solutes can occur. The first two factors are expressed by the safety functions relating to transport conditions in the buffer and the rock (Safety Functions R2a and b). The third factor is obtained by (i) an intact buffer in tight contact with the wall of the deposition hole, which, in turn, is achieved through the buffer swelling pressure (Safety Functions Buff1 and 2) , and (ii) limited aperture in the fractures intersecting the deposition hole (Safety Function R2a). The latter factor can increase considerably through thermally induced spalling of the rock wall of the deposition hole. A suitable indicator for this safety function is the equivalent flow rate, Qeq, which is an integrated measure of all the above factors. A low Qeq value implies the host rock having favourable hydrogeologic and transport conditions. SKB states that though it is not possible to put a quantitative limit on Qeq, as a rule of thumb values of Qeq below 10^{-4} m^3/yr can be regarded as favourable (TR-11-01, Section 8.3.4, page 260).

2.1.2. Treatment of Qeq in different time periods of the Safety Assessment

The SKB analysis focuses on estimating Qeq in the initial period of the temperate climate after closure (TR-11-01, Section 8.3.4). The excavation and operations phases could result in (i) development of Excavation Damaged Zone (EDZ), (ii) spalling, and (iii) reactivation of fractures. These factors, in turn, affect Qeq values and safety functions R2 a and b. These aspects are accounted for in the Qeq

analyses during the initial period of the temperate climate after closure. A detailed description of the Qeq analysis is provided in Section 2.1.3 of this report.

For the initial period of temperate climate after closure, the hydrogeological processes at the site are represented using a combination of Discrete Fracture Network (DFN) and continuous porous media models using a modelling tool (ConnectFlow) at the regional scale, repository scale and site scale (TR-11-01, Section 10.3.6, page 338). For each of the three repository blocks used in the repository scale model, the derived pressure solution is based on a discrete fracture network (DFN) medium representation of the fractured bedrock surrounding the repository. One of the outputs of the repository scale model is the equivalent flow rates (Qeq) at the deposition-hole positions.

During the remaining part of the reference glacial cycle, SKB does not expect significant changes to fractures located close to the deposition holes, but expects that Qeq will change due to the changing flow boundary conditions during the glacial cycle (TR-11-01, Section 10.4.11). SKB states that the advective flux in the fracture (q), more specifically the square root of q, controls the transport of corroding species from groundwater to the buffer. Flow rates are expected to increase between one and two orders of magnitude relative to the temperate climate as the ice front passes during advance and retreat. Relative to temperate values, flow rates are expected to be (i) generally slower during the phase when the repository is covered by ice, (ii) slower or at the same magnitude during permafrost, and (iii) much slower during submerged conditions. Sulphide concentrations, which SKB expects to drive copper corrosion rates, are expected to be similar or lower for periglacial or glacial conditions compared to those for temperate conditions. For intact buffer conditions, SKB concludes that corrosion has an insignificant impact on the copper canister thickness in a 120,000 year (one glacial cycle) perspective even if groundwater flow rates and sulphide concentrations for temperate conditions are assumed (TR-11-01, Section 10.4.9).

For the reference climatic evolution, the first glacial cycle is assumed to be repeated until the end of the one million year assessment period (TR-11-01, Section 10.5). Assuming a cycle period of around 120,000 years, results in a total of eight glacial cycles. For subsequent glacial cycles, irreversible phenomena related to Qeq such as buffer erosion, canister corrosion are essentially expected to occur to an extent eight times greater than that during the initial glacial cycle. SKB expects repetitions of the same pattern of variations in hydraulic gradients and small alterations of fracture transmissivity for different glacial loads as for the first glacial cycle (TR-11-01, Section 10.5.1). This implies that variation in groundwater flow and thus variations in Qeq values estimated during the initial glacial cycle will also be applicable for the subsequent glacial cycles. However, in deposition holes where advective conditions need to be assumed, Qeq should be replaced by the flow in the fracture intersecting the deposition hole. The evaluations of canister corrosion for the initial glacial cycle indicate that, for an unaltered buffer, corrosion would not cause canister failures even in a million years (TR-11-01, Section 10.5). For a buffer that has been partially eroded to the extent that advective conditions must be assumed in the deposition hole on average less than one canister may fail over the entire million year assessment period for this reason.

The global warming variant considers the combined effect of natural and anthropogenic climate change. This variant describes a future climate development influenced by both natural climate variability and climate change induced by anthropogenic emissions of greenhouse gases, with the latter resulting in weak to

moderate global warming. SKB concludes that the status of the safety function indicators at the end of a prolonged period of temperate climate can be expected to be very similar to those reported for the initial temperate period. The ability of the host rock to provide favourable hydrogeologic and transport conditions (Safety Function R2) is influenced by the flow rate at the buffer/host rock.

2.1.3. Detailed description of Qeq

SKB conceptualizes the conditions in the near-field as deposition holes being intersected by one or more fractures with flowing water (TR 10-42, Chapter 2). Diffusion is assumed to be the dominant mechanism of transport in the saturated intact buffer. SKB also states that molecular diffusion in the porous buffer carries solutes faster through the buffer than flow does because of the extremely small hydraulic conductivity of the buffer. However, advection is the dominant mechanism of flow in the fractures. SKB conceptualizes three main paths for transport of radionuclides from the waste canister to the fractures in the rock (Figure 1). SKB analyses indicates that for expected repository conditions the resistance to solute transfer between the host rock water and the buffer could be considerably larger than that in the buffer, thus limiting the overall rate of mass transfer.

The mass transfer between buffer and water in fractures is represented by an analytical model (TR 10-42, Chapter 2). The same model is also used to calculate the transport of corrosive agents to the canister. The same model is extended to a scenario that includes a damaged zone due to spalling with much higher hydraulic conductivity and porosity than the intact rock.

SKB introduced Qeq to facilitate understanding of how much solute (corrosive agent or nuclide) could be transported to or from the canister by the water seeping in the host rock (TR 10-42, Chapter 2). It can expressed as the flow rate of water that would be depleted of (filled with) its solute when the water passes the deposition hole. The rate of transport is proportional to the driving force (i.e., the concentration difference) and inversely proportional to a resistance ($R_{overall}$) to solute transfer. The overall resistance is expressed as a sum of resistances in the barriers through which the solute has to pass in series.

$$N = Q_{eq}^{overall}(c_w - c_o) = \frac{1}{R_{overall}}(c_w - c_o) = \frac{1}{\sum_i R_i}(c_w - c_o) = \frac{1}{\sum_i \frac{1}{Q_{eq,i}}}(c_w - c_o)$$

where N is the rate of exchange of a solute between the seeping water having a concentration c_w to a body (canister) that maintains its concentration at c_o. For the corrosion analysis, $c_o = 0$ if the corrosive agent immediately reacts with the copper canister. The same expression is used for release of a nuclide from the canister to the passing water, in which case c_o is radionuclide concentration inside the canister and c_w is concentration in the approaching water (assumed 0). For the corrosion analyses, Qeq for the transfer from the water seeping in the fractured rock to the outer surface of the buffer is determined by assessing how far out in the flowing water the solute can be depleted by diffusion during the time the water is in contact with the buffer (TR 10-42, Section 2.1). The flow and solute transport processes are modelled using Darcy's Law and Fick's Law. For the radionuclide release analyses,

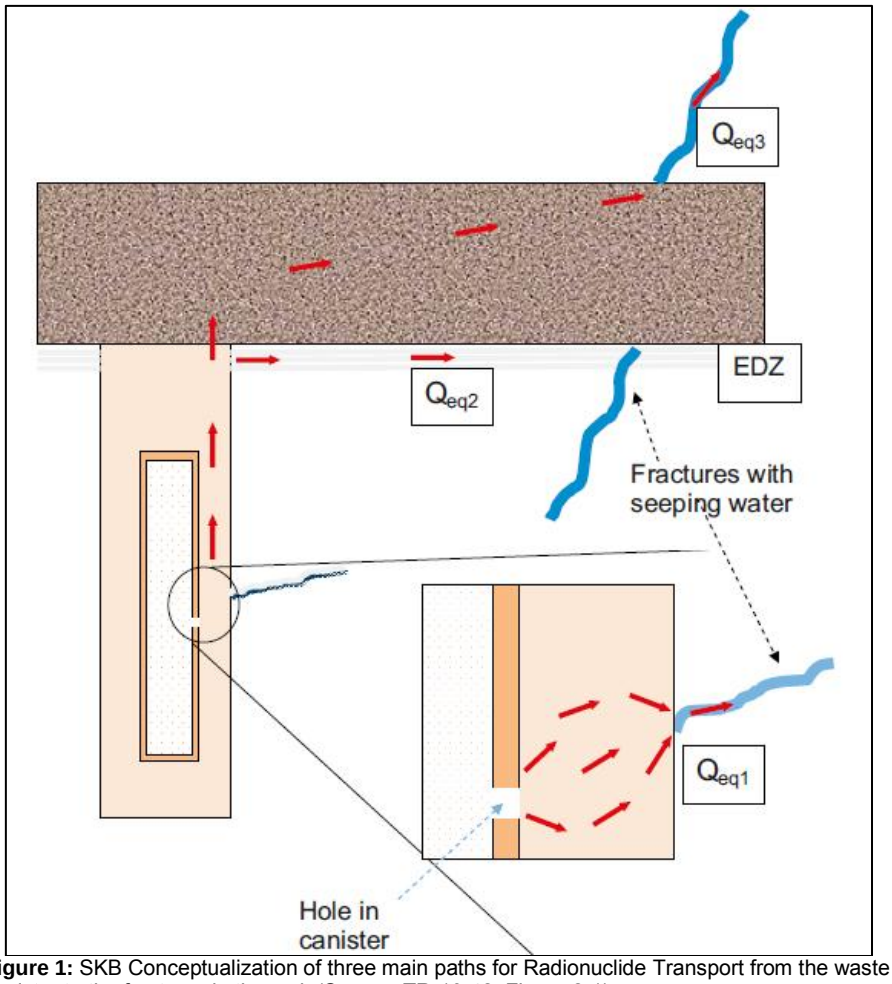

Figure 1: SKB Conceptualization of three main paths for Radionuclide Transport from the waste canister to the fractures in the rock (Source: TR-10-42, Figure 2-1).

the solute encounters a number of transport resistances (inverse of Qeq) in series and in parallel. The radionuclide must first diffuse from the fuel through a hole in the canister to the clay buffer, then diffuse through the buffer to reach the seeping water in the fracture in the rock. As the radionuclide approaches the fracture in the rock it will have to find the narrow fracture. This can also be expressed as a resistance. In a series of transport legs, the smallest Qeq (i.e., largest of the resistances in series) will have most impact on limiting the rate of transport to and from the canister. When the transport legs operate in parallel, the largest Qeq will have most impact on limiting the rate of transport to and from the canister.

Assumptions related to Qeq Analyses

SKB made several assumptions related to flow and transport processes in the Qeq analysis (TR 10-42, Section 7.2). They include:

- **Steady state.** The water flow rate in the fracture is assumed constant over time. This assumption is supported by estimating the characteristic time required for building up a steady-state concentration profile (t_{ss}) compared to the time it takes for flow rate or concentration to change. Analysis indicates that t_{ss} = 30 years that includes a spalled drift case. SKB asserts that the expected conditions at the repository will not involve flow rates or

concentrations to change more rapidly than in estimated t_{ss} of 30 years and hence supports the validity of the steady-state assumption. For the flow around the buffer in the fracture, a characteristic time can be taken as the time to practically saturate the water at a distance on the order of the radius of the deposition hole at most. This distance is approximately that which sets the validity of the model with Peclet Number (Pe) >4. The same approach can be used for the transport of radionuclides but the retardation due to sorption and nuclide decay must be accounted for. SKB estimated that t_{ss} ~50 RNu years for a buffer thickness of 0.4 m, where RNu is the retardation factor for the radionuclide. Retardation factors can be much larger than 1 for many sorbing nuclides, for which the steady state approximation may be violated. Similarly, nuclides with half-lives shorter than t_{ss} will also violate the assumption. SKB indicates that full transient calculations must be made when the assumption is violated.

- **Laminar flow and mixing by diffusion.** The assumption that the flow is laminar in the fractures and in the damaged zone is the basis for the use of molecular diffusion as the sole mechanism of solute mixing between streamlines. SKB estimates that Reynold's number (Re) is less than approximately 0.01 even for the highest reasonable transmissivity and gradient, ensuring laminar flow. Similarly the flow in the damaged zone and degraded concrete is also assumed to be laminar as the water velocity is lower in the multitude of fractures in the zone.
- **The solute concentration at the buffer/water interface is the same everywhere at the interface.** The assumption that the concentration at the interface is constant introduces an error that depends on the buffer geometry and relative diffusivities in water and buffer. This error is quite certainly less than what is due to the uncertainties in fracture aperture, fracture aperture variations flow rates etc. SKB concludes that it is not necessary to make a more detailed analysis of this assumption.

SKB analyses includes other assumptions such as (i) the fractures are narrow enough that the viscous boundary layer can be neglected when calculating solute advection along the buffer/rock interface, (ii) buffer does not expand into the fractures, (iii) diffusion through the rock matrix to and from the buffer is negligible compared to the other transport paths, and (iv) flow velocity in the damaged zones and in the concrete is spatially invariant (i.e., there are no channels with higher flow). SKB asserts that the assumption that no buffer has expanded out in the fractures is conservative because this process would strongly decrease the overall mass transfer due to the presence of an additional barrier. SKB agrees that, in reality, very strong channelling is expected in both regions. Then much or even most of the water will have a considerably lower residence time than the mean and mass transfer will be lower in the damaged zone as well as in the concrete. SKB asserts that the plug flow model is conservative with respect to channelling.

Cases included in the Qeq Analyses

SKB analyzed several cases to evaluate Qeq including

Case A: Mass transfer in an intact buffer interacting with a single fracture

SKB uses analytical solutions to evaluate (i) constant aperture fractures intersecting the deposition hole at right angles and (ii) fractures intersecting the deposition hole at an arbitrary angle. Processes in rough and variable aperture fractures are included (TR 10-42, Chapter 3). Figure 2 shows a canister deposition hole intersected by a fracture with seeping water as viewed from the side and from above. Water flows around the deposition hole because of the lower hydraulic conductivity of the intact buffer. The radionuclide transport process is illustrated with a nuclide that has penetrated through the buffer and is released into the water. The nuclide has reached and maintains a steady state concentration at the interface between the buffer and the water. Under repository conditions the flow is assumed to be laminar and the nuclide moves by molecular diffusion into the water. It diffuses further and further out into the water as the water moves along the buffer/water interface. The water picks up more and more nuclide along its path around the deposition hole. From diffusion theory we can determine the amount of nuclide that the water has carried away. In case of the corrosion process the process is reversed (i.e., a corrosive agent) (e.g., sulphide) is carried by water in fracture and migrates into the buffer. Analytical solutions are used to estimate the water flow rate, velocity and residence time. SKB analyses for a fracture inclined at an angle of 45° and vertical intersection resulted in a 10% and 44% increase in Qeq respectively (TR 10-42, Section 3.6). SKB states that the stream line disruption in case of a vertical fracture intersecting the deposition tunnel, which was not accounted in the analyses, could decrease Qeq. SKB asserts that it expects “no more than a few tens of % increase of Qeq at most” and concludes that the uncertainty in flow directions is thus marginal in the safety and performance assessment of a deep repository for spent nuclear fuel.

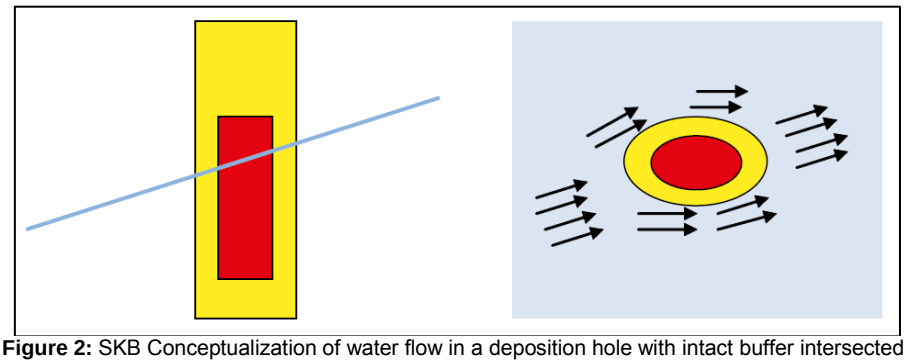

Figure 2: SKB Conceptualization of water flow in a deposition hole with intact buffer intersected by a fracture with flowing water as viewed from the side (left) and from above (right) (TR-10-42, Figure 3-1)

Case B: Mass transfer in a damaged rock wall in the deposition hole and in a degraded concrete bottom plate

Presence of damaged zones results in increased flow into the zone and to a longer residence time in contact with the buffer and in turn, increase in solute transport rate (TR 10-42, Chapter 4). SKB states that the tunnels will be aligned in the direction of highest horizontal stress. Any spalling damage will occur on the sides of the deposition hole perpendicular to that direction (Figure 3). Field measurements indicate that the increased hydraulic conductivity of damaged zone will imply reduced resistance to flow in this zone. SKB analysis assumed that fracture intersects the deposition hole at some angle and that water is drawn in on one side of the intersection with the damaged zone and out on the other. Given the larger hydraulic conductivity of the damaged zone, the transmissivity of the fracture limits the flow rate through the zone. It was shown that the water spreads out upward and downward along the zone in its passage. The water is effectively in contact with the buffer over only a fraction of the damaged zone. The residence time is also shorter than if it had access to all the pore space in the zone. The analysis was extended to a case where there also is a conductive region at the bottom of the deposition hole. This could be caused by chemical degradation of the concrete foundation at the bottom of the hole, which is cast to ensure that the bottom is level and smooth. The flow path is conceptualized such that water can flow into the damaged zone, down to the bottom of the deposition hole where the concrete bottom plate has been degraded and up the zone on the other side of the hole (Figure 3). The water flowing in these damaged zones will have a longer contact time with the buffer than what it would have without the presence of the damaged zones. Because of the significant difference in mass transfer properties and geometries of the damaged zone and the concrete SKB assumed that the mass transfer takes place in two different parallel paths that do not influence each other.

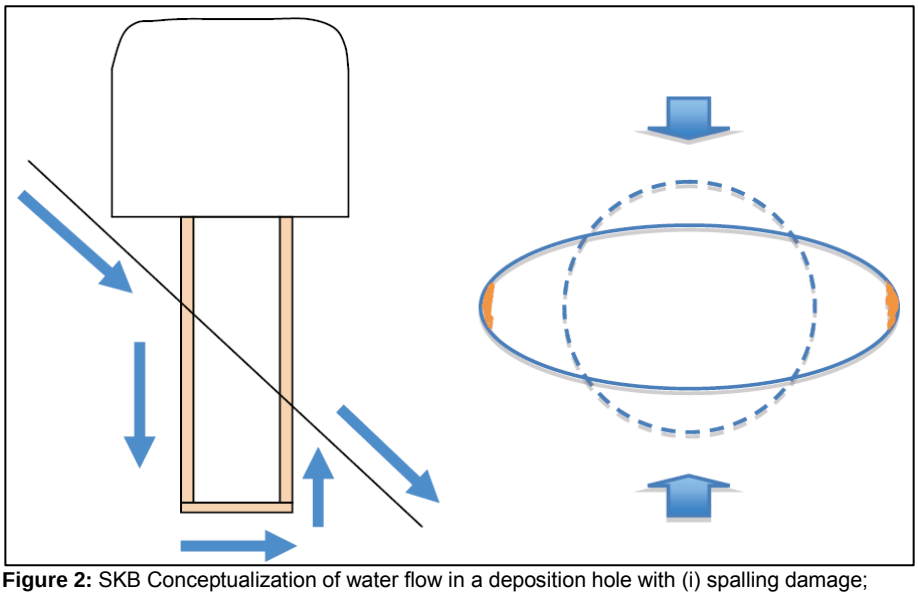

Figure 2: SKB Conceptualization of water flow in a deposition hole with (i) spalling damage; and (ii) a degraded concrete bottom plate that intersects a fracture. Blue Arrows indicate possible flow paths. The right picture shows how spalling occurs, marked orange, when the hole is compressed by rock stresses. (TR-10-42, Figure 4-1)

Case C: Mass transfer in the buffer and a damaged canister

SKB considered several aspects of the mass transfer analysis including (i) a large buffer area in contact with a damaged zone and degraded concrete, (ii) a very small fracture area exposed to the buffer, (iii) a small cylindrical defect in the canister, (iv) diffusion from a small hole in the canister into a large buffer volume, and (v) impact of a fractured cemented buffer on corrosion (TR 10-42, Chapter 5). For case (ii), the solute has to diffuse over the very small area of the fracture as it intersects the buffer. Similarly, a solute that diffuses through a small hole in the canister will expand out into the buffer before it converges to enter the narrow fracture in the rock and contacts the water (Figure 4). The solute that emerges from (or converges to) the fracture into the large volume of the buffer will encounter an increasingly larger (or smaller) cross section to diffuse through. The resistance to transport will decrease the farther from the fracture the solute has migrated. Most of the resistance is near the fracture mouth. SKB example calculations indicate that Qeq for transport through a small cylinder is one to two orders of magnitude smaller than Qeq for transport from the hole to the buffer, which in turn is 1.5 to 3 orders of magnitude smaller than Qeq from the buffer to fractures or degraded concrete. SKB assumes that canister resistance becomes ineffective after 10,000 years. For case (v), SKB analyzed the consequences of a crack (which forms because of a cemented buffer) that extends all the way through and connects to the fracture in the rock. The major impact is that the seeping water now comes in direct contact with the copper canister and can deliver any corrosive agent directly to the surface of the copper canister. SKB analysis indicates that the corrosive agent will react in the very narrow region where the crack is in contact with the canister and corrosion would be localized (TR 10-42, Section 5.5).

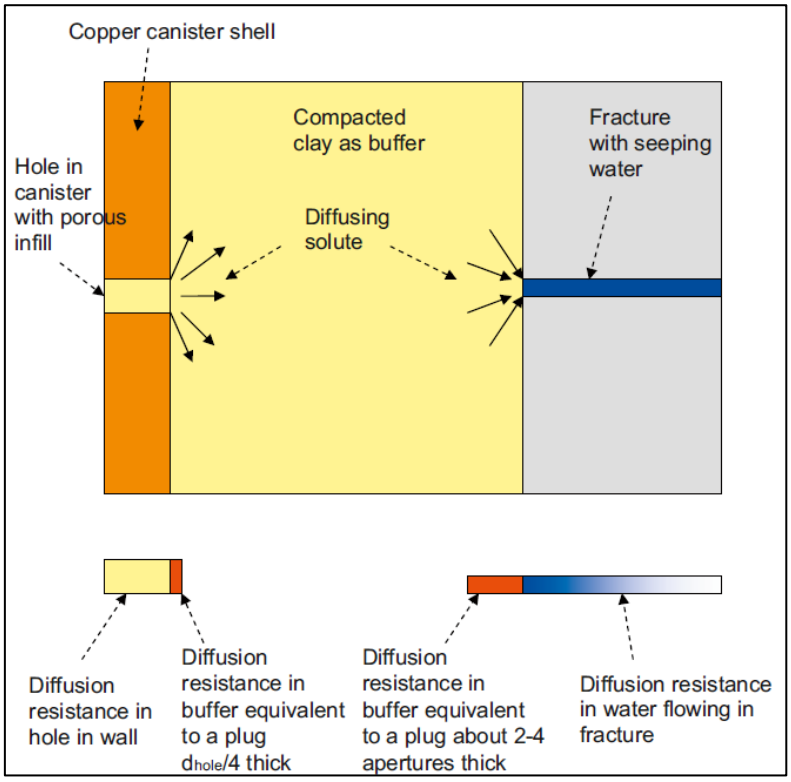

Figure 3: SKB conceptualization of mass transfer from the waste canister to the host rock (TR-10-42, Figure 5-1)

Case D: Qeq for flow in a partially eroded buffer

SKB states that the water that flows in the eroded volume around the canister will deposit a solute migrating to the canister or take up a solute from the canister by molecular diffusion (TR 10-42, Appendix). The longer the water is in contact with the canister, the more solute can be transferred. SKB used a simplified model to quantify the Qeq for this system assuming (i) canister and rock curvature are straightened out (flow is linear), (ii) the system is symmetric in the direction along the canister perpendicular to flow, (iii) temporal variation of concentration is neglected, and (iv) diffusion in the flow direction is neglected (Figure 5). These assumptions and simplifications result in accounting only for the residence time of water. SKB states that when the penetration depth of the solute into the water is small compared to the distance along the path the error introduced is small. When the penetration depth of the solute is large and reaches the rock wall most of the water will be equilibrated and longitudinal diffusion will not further influence the solute transfer. SKB asserts that the errors introduced are deemed be marginal considering the geometrical simplifications and other assumptions.

SKB provided estimates of individual and overall Qeq for example calculations using typical values expected for the repository. SKB indicates that by far the largest resistance to radionuclide escape is the leg consisting of the cylindrical hole through the canister.

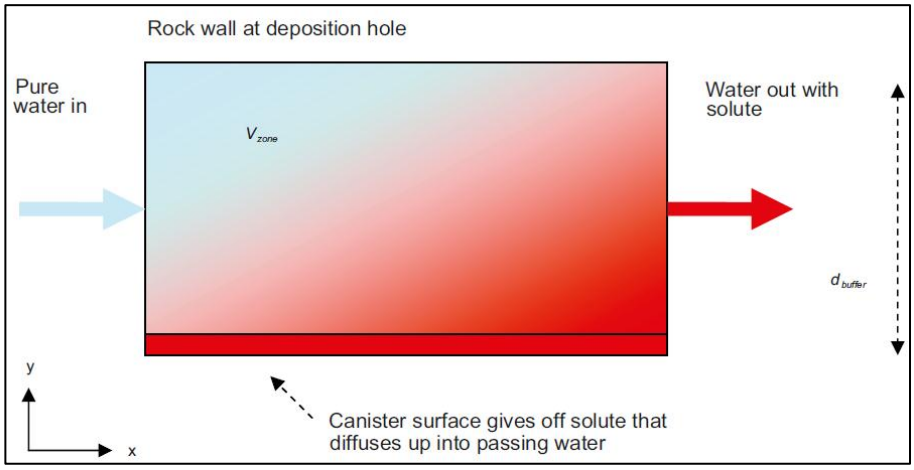

Figure 5: SKB conceptualization of mass transfer from the canister surface to the rock through the eroded buffer (TR-10-42, Figure A-1)

2.1.4. Implementation of the Qeq concept for copper corrosion calculations

SKB corrosion analysis involves calculation of the diffusive transport of corrodants through the buffer, accounting for the significant reduction in flow at the buffer-rock interface using the Qeq approach (TR-10-66, Chapter 4). The cases considered for the corrosion analysis include (i) an intact buffer with advection in fracture of the host rock, (ii) an intact buffer with a thermally induced spalling zone in the deposition hole, and (iii) partially eroded buffer with advection in the fracture.

Intact buffer with advection in a fracture

The Qeq modeling approach described in the previous section (i.e., TR-10-42) is implemented in the SKB corrosion analyses to describe the transport of sulphide towards the waste canister. The transport resistance in the case of a fractured rock consists of the transport from the fracture to the buffer ($1/Q_{eqhydro}$) in series with the transport in the buffer, geometrically taking into account that the sulphide is spread out in different directions in the bentonite ($1/Q_{eqgeometric}$) (Figure 6) (TR-10-66, Section 4.2). The ($1/Q_{eqgeometric}$) factor represents the transport resistance for the mass transfer in buffer when a very small buffer area is exposed to the solute in the flowing groundwater. The solute that goes from the fracture will encounter an increasingly larger cross section to diffuse through and the resistance decreases the farther from the fracture the solute has diffused. This could also be seen as a spreading of the solute in the bentonite. SKB analysis showed that for typical KBS-3 dimensions, this resistance can be described as equal to that in a thin band at the mouth of the fracture. The area of the band is set equal to the fracture opening and the band thickness (extension into the buffer) to a distance about 2–4 times the fracture aperture. This resistance can be represented by a plug resistance all around the fracture intersection. The area of the plug, A_{plug}, is the fracture opening area. The length of the plug, l_{plug}, is the band thickness.

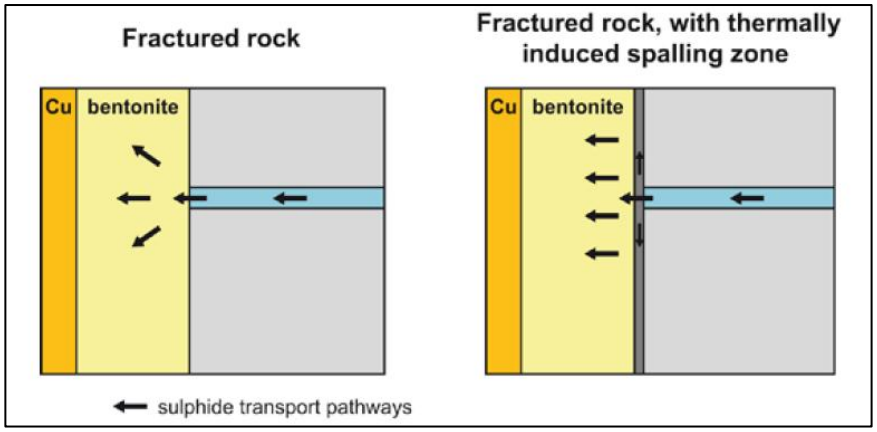

Figure 6: SKB conceptualization of transport pathways for sulphide for a fractured rock and for fractured rock with a thermally induced spalling zone. (TR-10-66, Figure 4-1)

$$R = \frac{1}{Q_{eqhydro}} + \frac{1}{Q_{eqgeometric}}$$

where

$Q_{eqhydro}$ is Qeq taken from the output of the hydrogeological DFN model for each deposition hole for SR-Site and

$$Q_{eqgeometric} = \frac{D_{e,buffer,i} A_{plug}}{l_{plug}}$$

where
$D_{e,buffer,i}$ is effective diffusion coefficient in the buffer for species i
A_{plug} is area of the plug = 5.5E-4 m^2
l_{plug} is length of the plug = 3.1E-4 m.

For the case with a thermally induced spalling zone the transport directly from the fracture to the buffer ($Q_{eqhydro}$) is the same as without spalling, but in parallel to

transport path through the damaged zone (Figure 6). This combined transport resistance is in series with the diffusion perpendicular through the buffer to the canister surface.

$$R = \frac{1}{Q_{eqhydro} + Q_{eqspalling}} + \frac{1}{Q_{eqdiffusive}}$$

$$Q_{eqspalling} = 1.13\sqrt{\frac{D_w q_{zone} W_{zone} L_{zone} \varepsilon_{zone}}{d_{zone}}}$$

$$Q_{eqdiffusive} = \frac{D_{e,buffer,i} W_{zone} L_{zone}}{d_{buffer}}$$

where

D_w is diffusion coefficient of solute in water
q_{zone} is flow rate in the spalling zone (see TR-10-66, Section 4.2, page 18 for additional details)
L_{zone} is length of the spalling zone
d_{zone} is thickness of the spalling zone
ε_{zone} is porosity of the spalling zone
W_{zone} is width of the spalling zone
d_{buffer} is thickness of the buffer

SKB also suggests a more pessimistic approach where all the water in the spalled zone is equilibrated so that Qeq = q_{zone} (TR-10-66, Section 4.2.1). The total resistance for the case including spalling using this pessimistic assumption is

$$R = \frac{1}{Q_{eq}} = \frac{1}{q_{zone}} + \frac{1}{Q_{eqdiffusive}}$$

Based on the Qeq values, the transported amount of solute (sulphide) is calculated as follows (TR-10-66, Section 4.2.2)

$$N_{HS} = Q_{eq} \cdot [HS^-] \cdot t$$

where

N_{HS} is amount of sulphide
$[HS^-]$ is concentration of sulphide in groundwater
t is time considered

The general expression for the highest corrosion rate at the canister side is

$$v_{corr} = BCF \cdot Q_{eq} \cdot [HS^-] \frac{f_{HS} M_{Cu}}{2\pi r_{can} h_{can} \rho_{Cu}}$$

where

BCF is buffer concentration factor = 7
f_{HS} is stoichiometric factor for reaction with sulphide = 2
M_{Cu} is molar mass of copper = 63.55 g/mole
r_{can} is radius of the canister = 0.525 m
h_{can} is height of the canister = 4.835 m ~ 5 m

ρ_{Cu} is density of copper = 8,920 kg/m^3

For the spalling case,

$$v_{corr}^{spalling} = Q_{eq} \cdot [HS^-] \frac{f_{HS} M_{Cu}}{W_{zone} L_{zone} \rho_{Cu}}$$

Partially eroded buffer with advection in a fracture

The Qeq modelling approach described in the previous section (i.e., TR 10-42, Appendix) is implemented in the SKB corrosion analyses to describe the transport of sulphide towards the waste canister. For a wide range of conditions the equivalent flow rate, Qeq, used for assessing the migration of corrodants from the groundwater to the canister should be replaced by q_{eb}, the water flux through the part of the fracture that intersects the deposition hole. For high flow rates though (i.e. for $q_{eb} > q_{lim}$), Qeq can be approximated as follows

$$Q_{eq} = 1.13 \frac{\sqrt{V_{zone} D_w q_{eb}}}{d_{buffer}}$$

$$q_{eb} = f_{conc} U_0 2 r_h h_{can}$$

$$V_{zone} = \frac{h_{zone} \pi (r_h^2 - r_{can}^2)}{2}$$

where

V_{zone} is volume of the eroded buffer
f_{conc} is flow concentration factor to account of the lost flow resistance in the eroded buffer (2)
U_0 is Darcy flux from the hydrogeological DFN modeling
r_h is radius of the deposition hole = 0.875 m
h_{zone} is height of the eroded zone ~ d_{buffer} = thickness of the buffer

SKB notes that the derived expression for the flow rate is valid for a horizontal fracture. If the fracture has a longer intersection with the vertical deposition hole than a horizontal fracture, then the flow rate will increase in proportion to the intersection length, but so will the buffer mass loss required for advective conditions and the exposed canister surface. Hence, the fracture angle does not impact erosion or corrosion results.

The corrosion rate for the eroded buffer case, similar to the intact buffer case, is derived as follows:

$$v_{corr} = Q_{eq} \cdot [HS^-] \frac{f_{HS} M_{Cu}}{\rho_{Cu}} \cdot \frac{1}{A_{corr}}$$
$$A_{corr} = \pi r_{can} h_{corr}$$

where

A_{corr} is area exposed to corrosion

h_{corr} is height of zone exposed to corrosion (variable – See TR-10-66 Section 4.3.3 for additional details)

For the cases considered in its corrosion analyses, SKB concludes that expected corrosion depth is much smaller than the copper shell thickness for a performance period of a million years (TR-10-66, Chapter 6). SKB notes that in the case of an eroded buffer and only for the deposition hole with the highest flow rate that the corrosion is in the millimetre scale. For the case of a partially eroded buffer, the probabilistic calculations show that corrosion could lead to penetration of the copper shell for on average less than one canister, for the assessment time of a million years. SKB analysis included the most unfavourable combinations of sulphide concentration and flow rates. The calculations accounted for the variability in the hydrogeological DFN models and uncertainties in the assumed sulphide concentration distribution, as well as uncertainties in the conceptual model of corrosion geometry (the part of the copper surface that is corroded by the sulphide transported to the canister) and resulted in 0 to less than 2 penetrated canisters.

Implementation of the Qeq concept for radionuclide transport calculations

Groundwater flow is a primary control on radionuclide migration in the subsurface. SKB identifies Qeq as one of the three main input parameters (flow triplet parameters) related to flow in its transport calculations (TR-10-50, Section 2.1). The remaining two parameters are the advective travel time t_w, and the flow-related transport resistance F. The flow triplet parameters vary spatially and by realization of the stochastically generated DFN. The Qeq varies by canister location, release path, and DFN realizations. The t_w and F parameters are properties of the flow path connecting a near-field release location to a geosphere discharge location. Thus, a unique pair of t_w and F is required for each combination of DFN realization, canister location, near-field release path, and flow path through the geosphere.

The transport calculations analyze consequences of the two scenarios identified as the most risk significant: canister failure due to corrosion and canister failure due to shear load. In the 'canister failure due to corrosion' scenario (also called as the corrosion scenario) canisters fail as a result of enhanced corrosion due to advective conditions in the deposition hole following the loss of buffer through erosion. In the 'canister failure due to shear load' scenario, canisters fail due to earthquake-induced secondary shear movement along fractures intersecting the canister position. In addition, several residual scenarios that help understand geosphere barrier function are also analyzed.

The three hydrogeological models (semi-correlated, uncorrelated and fully correlated) form the base for the transport calculations. The hydrogeological calculations are performed for different climate conditions. Temperate conditions at the time 2000 AD are assumed to provide adequate representations of near-field and far-field conditions at Forsmark for the purpose of estimating radionuclide release and transport. This approximation is relaxed in a few selected variant modelling cases to evaluate its adequacy.

In all the scenarios evaluated by SKB, except the corrosion scenario, the nuclides are sorbed with varying efficiency in the buffer and the diffusion and sorption properties determine the time for diffusion through the buffer to the rock at release path Q1 (i.e., a fracture intersecting the deposition hole). In the shear load scenario,

the shear is assumed to increase the fracture transmissivity significantly. The Qeq value for the intersecting fracture is assumed to be sufficiently high that it does not contribute to the transport resistance in the near field. In the two hypothetical residual scenarios, isostatic load and growing pinhole, the limited flow in the fractures intersecting the deposition hole contributes to the transport resistance through the Qeq value. Thermally induced spalling is assumed to have occurred in the wall of the deposition hole. This implies that the transport resistance at the interface at Q1 is lower than if spalling is not included. In the growing pinhole scenario, two additional exits from the near field are included: an EDZ in the floor of the deposition tunnel (if such a zone is assumed to exist), Q2, and a fracture intersecting the deposition tunnel, Q3 (Figure 7). The radionuclide transport is assumed to occur by diffusion in the buffer and backfill in the deposition hole and by diffusion and advection in the deposition tunnel. The nuclides are sorbed with varying efficiency in the buffer and backfill and the water flow, the diffusion and sorption properties in the backfill determine the time for diffusion through the buffer and backfill to the rock at release paths Q1, Q2 and Q3. The advective flow in the deposition tunnel and the boundary conditions for the near field at Q1, Q2 and Q3 are determined in the hydrogeological calculations.

SKB analysis relies on three numerical models for calculations of radionuclide release and transport (TR-10-50, Section 3.6). COMP23 is used for radionuclide migration calculations in the canister interior, the buffer and the deposition tunnel backfill (TR-10-50, Appendix G). COMP23 models (i) diffusion and sorption in the buffer and (ii) advection, diffusion and sorption in the deposition tunnel backfill. It also handles the release of radionuclides to different exit paths from the near field. SKB implements analytical solutions at sensitive zones to enhance calculation speed in COMP23, for example (i) at the exit point of a small canister hole and (ii) at the entrance to fractures. The radionuclide transport calculations in COMP23 are described in the following sections for several cases, including (i) a growing pinhole with and without spalling, (ii) loss of swelling pressure in tunnel backfill, (iii) canister failure due to shear load, and (iv) canister failure due to corrosion.

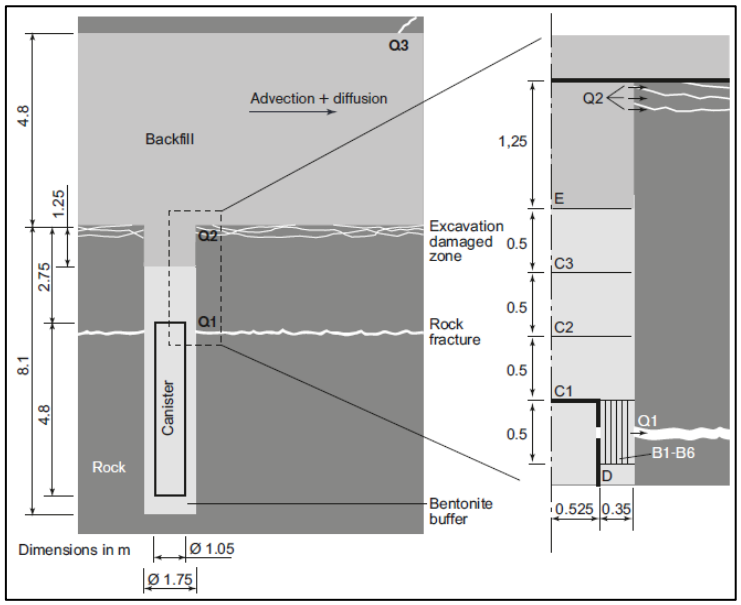

Figure 7: SKB's representation of near-field radionuclide transport processes in COMP 23 model for the growing pinhole scenario. The transport paths Q1, Q2 and Q3 to a fracture intersecting the deposition hole, to the excavation damaged zone, and to a fracture intersecting the deposition tunnel, respectively, are also shown. (Reproduced from TR-10-50, Figure 3-1).

Growing pinhole – no spalling

SKB's conceptualization of the transport path from a defective canister, through the buffer, and into flowing water in fractured rock, is shown in Figure 8. Three exits from the near field are included: (i) a fracture intersecting the deposition hole at the vertical position of the canister lid, denoted Q1; (ii) EDZ in the floor of the deposition tunnel, Q2; and (iii) a fracture intersecting the deposition tunnel, Q3. In the hydrogeological modelling, the number of fractures intersecting a deposition hole and the properties of these fractures are determined statistically based on the DFN description of the rock. If more than one fracture intersects a deposition hole, the transport capacity of the several fractures are added and pessimistically assigned to the single fracture, Q1, modeled by COMP23. The equivalent flow rate through Q2 is also calculated as an integral part of the hydrogeological modelling. The flow rate in the deposition tunnel (Q3) and the distance to the nearest fracture through which radionuclides are released to the geosphere from the tunnel are given by the hydrogeological modelling. Transport by advection and diffusion in the tunnel is included in the near-field simulations and the computational domain is extended in the downstream direction to include the Q3 fracture.

In COMP23, a 2D-cylindrical coordinate system was chosen with x-axis set along the radial and y-axis along the axial direction (TR-10-50, Section G2). The implementation in the COMP23 numerical code, schematically shown in Figure 9, consists of several blocks, plugs and boundary conditions. Detailed description of the dimensions (x and z) and flow directions for the blocks is available in TR-10-50, Section G2.

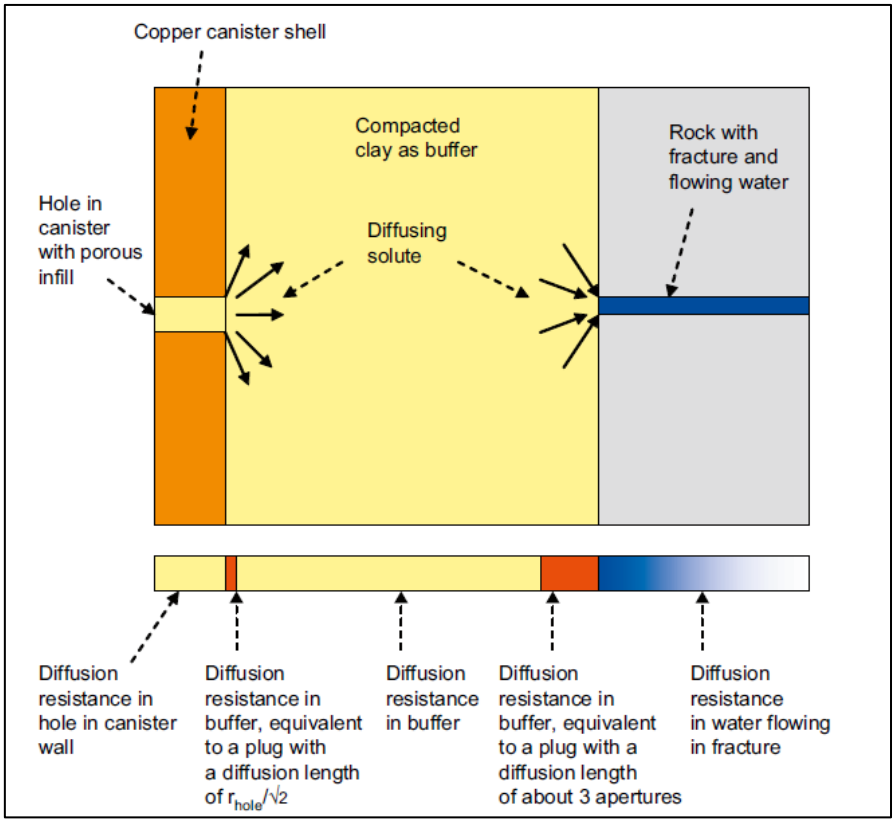

Figure 8: SKB conceptualization of the transport path from a defective canister, through the buffer and into flowing water in fracture rock (TR-10-50, Figure G-1)

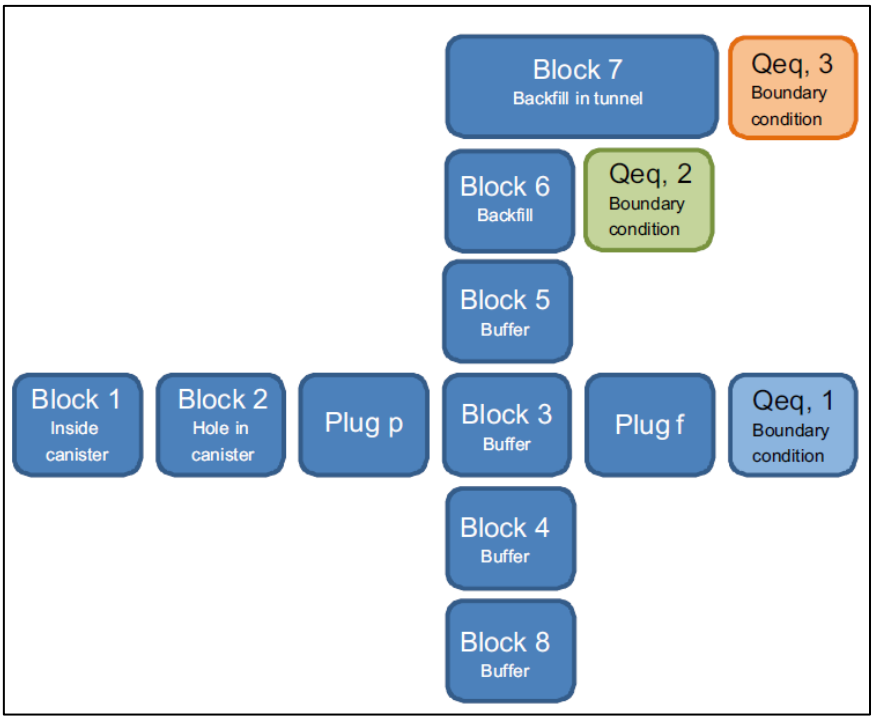

Figure 9: Schematic representation of SKB's COMP23 – a numerical code for radionuclide transport–for the case with growing pinhole failure without spalling. (Reproduced from TR-10-50, Figure G-2).

Transport from the hole into the buffer: An analytical model is used to represent transport through the hole in the canister. It is assumed that (i) species diffusing out from a circular hole spread out spherically and (ii) most of the resistance to diffusion is concentrated near the mouth of the hole. The resistance to diffusion is represented by a plug with a resistance, R_p, between the compartments representing the water in the hole and the buffer outside the canister and is calculated as

$$R_p = \frac{d}{AD_e} = \frac{1}{\pi r_{hole}\sqrt{2}D_e}$$

where

d is the diffusion length of the plug (m) (set equal to $r_{hole}/\sqrt{2}$)
A is the diffusion area (m^2) (approximately the area of the hole, A_{hole})
D_e is the effective diffusivity in the buffer (m^2/s)
r_{hole} is the radius of the hole (m)

Transport into a narrow fracture: Most of the resistance to transport will be located nearest to the fracture. The plug resistance at the fracture is represented using an analytical model that solves the steady-state two-dimensional diffusion equations for a sector of the buffer representing half the fracture spacing. The plug resistance, R_f is calculated as

$$R_f = \frac{\left(\frac{F_{x,0}}{b}\right) b}{A_f D_e}$$

where
b is the half-width of the fracture aperture (m)
A_f is the diffusion area (m^2) (set equal to the area of the fracture opening)
$F_{x,0}$ is the effective diffusion length function (m).

The effective diffusion length function ($F_{x,0}$) is calculated for plug connection with Q1 (see (TR-10-50, Section G2, page 303 for additional details). No additional resistance is used for connections with Q2 and Q3.

Advective flow: The advective flow in the tunnel is calculated as

$$q = \frac{L_{LR\_TUN}}{t_{TR\_TUN}} \in_{backfill} A_{tunnel}$$

where

L_{LR_TUN} is length of the tunnel from the top of the deposition hole to the first fracture intersecting the tunnel
t_{TR_TUN} is advective travel time from the top of the deposition hole to the first fracture intersecting the tunnel
$\in_{backfill}$ is porosity of the backfilled tunnel
A_{tunnel} is cross-sectional area of the tunnel

Boundary Conditions: The equivalent groundwater flow rates for pathways Q1, Q2, and Q3 is calculated using the Qeq-approach described in Section 2.1.3 of this report. The value of Qeq depends on the geometry of the contact area, the water flux, the flow porosity and the diffusivity. The Qeq-values are calculated within the hydrogeological modelling and directly used as input data to COMP23. Most of the values were determined in the hydrogeological models unless otherwise noted.

Equivalent groundwater flow rate, Qeq1:

$$Q_{eq1} = \sum_f \frac{Q_f}{\sqrt{a_f}} \sqrt{\frac{4 D_w t_{wf}}{\pi}}$$

$$t_{wf} = \frac{L_f \cdot e_{tf}}{Q_f / \sqrt{a_f}}$$

If there are several fractures intersecting a single deposition hole, then SKB uses a conservative approach to calculate the equivalent groundwater flow rate that sums up the flows across all the fractures, with t_{wf} calculated separately for each fracture. The average equivalent flux, U_{r1}, for all fractures intersecting a deposition hole is

$$U_{r1} = \frac{1}{w_c} \sum_f \frac{Q_f}{\sqrt{a_f}}$$

where

D_w is the diffusivity in water [0.0316 m^2/yr]
t_{wf} is the time the water is in contact with the deposition hole within each fracture [yr]
L_f is the length of the fracture intersection with the wall of the deposition hole [m]

U_{r1} is the equivalent initial flux in the fracture system averaged over the rock volume adjacent to the deposition hole [m/yr]
Q_f is the volumetric flow rate in the fracture intersecting the deposition hole [m^3/yr]
e_{tf} is the transport aperture of the fracture intersecting the deposition hole [m]
a_f is the area of the fracture plane intersecting the deposition hole [m^2]
w_c is the deposition hole height [5 m].

Equivalent groundwater flow rate, Qeq2:

$$Q_{eq2} = \sum_E \frac{Q_E}{\sqrt{a_E}} \sqrt{\frac{4D_w t_{wE}}{\pi}}$$

$$t_{wE} = \frac{L_E \cdot e_{tE}}{Q_E / \sqrt{a_{fE}}}$$

The average equivalent flux, U_{r2}, for all fractures intersecting a deposition hole is

$$U_{r2} = \frac{1}{w_E} \sum_E \frac{Q_E}{\sqrt{a_E}}$$

where

t_{wE} is the time the water is in contact with the deposition hole within each EDZ fracture [yr]
L_E is the length of the EDZ fracture intersection with the wall of the deposition hole [m]
U_{r2} is the equivalent initial flux in the EDZ fracture system averaged over the EDZ fracture cross-sectional area [m/yr]
Q_E is the volumetric flow rate in the EDZ intersecting the deposition hole [m^3/yr]
e_{tE} is the transport aperture of the EDZ intersecting the deposition hole [m]
a_E is the area of the EDZ fracture plane intersecting the deposition hole [m^2]
w_E is the EDZ thickness [0.3 m].

Equivalent groundwater flow rate, Qeq3

$$Q_{eq3} = 2\sqrt{\frac{4D_w L e_{tf}\left(Q_f / \sqrt{a_f}\right)}{\pi}}$$

The initial flux, U_{r3}, for flow in the first fracture intersecting the tunnel is

$$U_{r3} = \frac{Q_f}{w_T \sqrt{a_f}}$$

where

L is the half circumference of the tunnel [7 m]
Q_f is the volumetric flow rate in the fracture intersecting the tunnel [m^3/yr]
e_{tf} is the transport aperture of the fracture intersecting the tunnel [m]
a_f is the area of the EDZ fracture plane intersecting the deposition hole [m^2]
w_T is the fracture width intersecting the tunnel [2.5 m].

At the upstream boundary for advective transport, the concentration is zero and no diffusion is allowed. At the downstream boundary, the radionuclides are transported out of the model with no diffusion. The additional advective component is given by

$$Q_{eq3,adv} = \frac{L_{LR\_TUN}}{t_{TR\_TUN}} \epsilon_{backfill}\, A_{tunnel}$$

The resistances for the compartments are calculated as

$$R = \frac{d}{AD_e}$$

where

d is diffusion length (m)
A is diffusion area (m^2)
D_e is material and nuclide specific effective diffusivity (m^2/yr) (probability density functions)

The COMP23 algorithm for calculating the network in Figure 9 considers a series of resistances from the canister interior to the respective outlet:

The total resistance for diffusion from canister through the boundary at Q1:

$$R_{TOT\ Q1} = R_{Block1} + R_{Block2} + R_{Plug\ p} + R_{Block3,horiz} + R_{Plug\ f} + \frac{1}{Q_{eq,1}}$$

The total resistance for diffusion from canister through the boundary at Q2:

$$R_{TOT\ Q2} = R_{Block1} + R_{Block2} + R_{Plug\ p} + R_{Block3\ vert} + R_{Block5} + R_{Block6\ verthoriz} + \frac{1}{Q_{eq,2}}$$

The total resistance for diffusion from canister through the boundary at Q3

$$R_{TOT\ Q3} = R_{Block1} + R_{Block2} + R_{Plug\ p} + R_{Block3\ vert} + R_{Block5} + R_{Block6\ vert} + R_{Block7} + \frac{1}{Q_{eq,3}}$$

Blocks 3 and 6 are subdivided into compartments. TR-10-50 (Appendix G.2) describes how the resistances in these compartments are calculated in series or in parallel.

Growing pinhole – with spalling

The model for the growing pinhole failure including the effect of spalling (i.e., a damaged zone in the rock walls of the deposition hole), is similar to the model without spalling (TR-10-50, Section G2) with three differences: (i) the plug at the inlet to the fracture is not present, (ii) the resistance in the half of the last buffer compartment next to the rock is included, and (iii) calculation of Q_{eq1} includes an additional term (Q_{eqDZ}) to account for the effect of the damaged zone.

Q_{eqDZ} is calculated as follows

$$Q_{eqDZ} = 1.13\sqrt{\frac{D_p q W_{zone} L_{zone} \varepsilon_{zone}}{d_{zone}}}$$

$$q = w_c U_0 \min[2L_{zone}, L_{fracture}]$$

where

D_p is pore diffusivity in the damaged zone (10^{-11} m^2/s)
q is water flow rate (m^3/s)
W_{zone} is width of the damaged zone (0.5 m)
L_{zone} is length of the damaged zone (8 m)
ε_{zone} is porosity of the damaged zone (0.02)
d_{zone} is thickness of the damaged zone (0.1 m)
U_0 is water flux from the hydrogeological model (m^3/m^2s)
w_c is canister height (5 m)
$L_{fracture}$ is length of the fracture intersecting the damaged zone

Loss of swelling pressure in the tunnel backfill

If the swelling pressure of the deposition tunnel backfill is lost, a conductive channel could develop at the tunnel ceiling. A simplified tunnel discretization is used for this case (TR-10-50, Section G4). The backfill is represented with only the backfill straight above the deposition hole. All blocks, except Block 7, are unchanged compared to the growing pinhole with spalling (Figure 9). One additional block is used, Block 8, representing the water at the tunnel ceiling. Block 9 is the same as the growing pinhole Block 8. Block 7 is modified to be only the backfill in the tunnel above the deposition hole.

Canister failure due to shear load

The canister failure due to rock shear load is caused by a large earthquake in the vicinity of the repository. The radionuclide release calculations include (i) the resistance for the diffusion from the "slit" in the sheared canister into the buffer, (ii) a resistance at the entrance to the fracture, and (iii) a limited Qeq1 value. The bentonite thickness is assumed to be reduced from 35 to 25 cm. SKB uses a simplified "pessimistic model" to represent the shear aperture in the canister and the fracture aperture in this analysis. The canister failure location is assumed to fully coincide with the location of the shearing fracture. The shear is assumed to increase the fracture significantly. The $Q_{eq,1}$ value for the intersecting fracture is assumed to be sufficiently high, $1 m^3/yr$, that it does not contribute to transport resistance.

Canister failure due to corrosion

When the canister failure is due to corrosion, it is assumed that there is no diffusion resistance in the near field. The flow into the deposition hole is calculated using

$$u = f_{conc} U_0 2 r_h h_{can}$$

where

f_{conc} is flow concentration factor (2)
U_0 is Darcy flux calculated by the hydrogeological model
r_h is radius of the deposition hole (1.75 m)
h_{can} is the height of the canister (5 m)

The output of COMP23 is used by FARF31, which performs radionuclide migration calculations in the far field (geosphere), and MARFA, which is used to simulate the transport of radionuclides and is specifically designed to integrate with the safety assessment workflow used by SKB (TR-10-50, Section 3.6).

SKB summarizes the near-field and far-field maximum dose-equivalent releases for probabilistic numerical calculation cases in TR-10-50 (Section 7). SKB notes that for the corrosion cases and shear load cases, the maximum normally appears at one million years while pinhole cases and isostatic load cases, in general, have their maximum shortly after the large failure in the canister. For all probabilistic cases considered by SKB, the maximum over the one million year assessment time of the mean total far-field effective dose is smaller than the dose corresponding to the risk limit. Excluding hypothetical cases (e.g., growing pinhole and postulated failure at 100,000 years due to shear load) and the cases supporting the discussion of best available technique, the far-field effective dose is at least one order of magnitude smaller than the dose corresponding to the risk limit. The two scenarios contributing to the calculated risk (i.e., failure of the copper canister by corrosion and earthquake-induced shear failure of the copper canister), the peak of the mean annual effective dose is estimated to be 0.18 μSv/yr and 0.15 μSv/yr, respectively. These doses, which assume reference conditions, could be compared with the dose corresponding to the risk limit of 14 μSv/yr and the dose corresponding to typical background radiation of approximately 1,000 μSv/yr.

2.2. Motivation for the assessment

The Swedish Radiation Safety Authority (SSM) has completed the initial review phase of SR-Site, the safety analysis submitted by SKB. SSM concluded from the initial phase of review that SKB's reporting is sufficiently comprehensive and of sufficient quality to justify a continuation of SSM's review to the main review phase. During the main review phase, SSM has developed technical review assignments that consider one or several specific issues or areas that SSM deems to require detailed assessment.

SSM intends this technical review assignment to (i) consider how the entity Qeq is calculated, (ii) assess if the results and cases SKB has chosen are relevant as input to the calculation of copper corrosion and radionuclide transport, and (iii) assess the relevance of the implementation of the Qeq concept for copper corrosion calculations.

SKB uses the Qeq concept in the context of near-field transport of dissolved species. SKB considers near-field transport for two purposes: (i) copper canister corrosion and (ii) radionuclide release. In our opinion, the Qeq parameter is so intimately linked with near-field transport that assessment of the Qeq parameter is essentially the same as assessing the SKB near-field transport approach, at least with respect to the interaction of flow and diffusive transport. Therefore, we addressed the technical review assignment by considering the following tasks: (i) summarizing

SKB's near-field transport methodology and identifying risk-significant aspects, (ii) independently testing risk-significant aspects of the model, and (iii) identifying any potential weaknesses in the safety case with respect to near-field transport, in particular canister corrosion.

2.3. The Consultants' assessment

2.3.1. Assessment overview

SKB uses the Qeq concept in the context of near-field transport of dissolved species. SKB considers near-field transport for two purposes: (i) copper canister corrosion and (ii) radionuclide release. In both contexts, SKB considers transport as a series of diffusion legs. SKB also considers several diffusion legs in parallel for release calculations. SKB uses a mixture of analytical approaches to represent diffusion for (i) different geometries and (ii) different flow conditions, combining these different conditions into a single parameter for each leg, which SKB calls Qeq. SKB calculates total mass flux along a pathway by multiplying Qeq by the difference in concentration across the pathway. The Qeq parameter, which combines a diffusion coefficient with spatial factors (e.g., diffusion area, diffusion length, boundary conditions), has dimensions of volume per time. SKB interprets the Qeq parameter as both the inverse of a resistance and as an equivalent volumetric flux.

SKB spreads the Qeq concept through several documents related to near-field transport. For our assessment, we focused on the rationale for the approach (TR-10-42) and applications to corrosion (TR-10-66) and radionuclide transport (TR-10-66), but the approach is discussed in several higher-level documents as well. Because of the use of the concept across several documents, the SKB presentation can be difficult to follow for a casual reader. We had initial difficulty with understanding the SKB presentation because (i) the SKB terminology has persistent connotations that advection is part of the Qeq concept, and (ii) SKB presents a myriad of special cases to describe different geometries and flow conditions. SKB persistently describes the Qeq parameter in terms of both resistance and volumetric flux, and we found SKB's interpretation of diffusion in terms of a volumetric flux to be unusual for nuclear repository and groundwater transport applications. Describing the Qeq parameter in terms of volumetric flux carries the connotation of (at least an equivalent) advective transport rather than diffusive transport, because the advection/diffusion equation typically used for transport calculations applies volumetric flux in the context of advection. Adding further overtones of advection into a purely diffusive context, SKB considers diffusion legs within flowing water, a context in which advection is important.

Once we understood the terminology, it became clear that the SKB approach for near-field transport is a network model for steady linear diffusion in a series of a few sequential and parallel diffusion legs, using a variety of analytical methods to calculate different geometric factors. This type of problem is common across many fields of mathematical physics; SKB points out the analogy to resistance networks in electrical circuits. Network models, when applicable, are attractive for stochastic modelling because network models are computationally efficient relative to typical partial differential equation methods. With this conceptual understanding of the Qeq concept to unify the different threads, we were able to place the SKB approach in context.

We conclude that SKB is using a consistent and logically straightforward framework, based on widely applied approaches, to model diffusive near-field transport.

The context of the SKB network approach for near-field transport, together with the peculiarities of the canister, buffer, deposition hole, and host rock, immediately imply that several types of diffusion legs are necessary to account for particular diffusion geometries. Some diffusion legs use the reasonable approximation of being essentially one-dimensional; other legs represent radially converging or diverging diffusion related to pinholes and fracture traces contacting the buffer, and diffusion into flowing water adjacent to a stagnant reservoir. As part of our assessment, we examined the theoretical underpinnings for the different types of legs.

We conclude that SKB is using reasonable and appropriate methods to develop approximations for the legs, based on our understanding of numerical methods.

Conceptual understanding of the approach

The Qeq approach considers steady-state diffusion across multiple legs, implying that the response time within the near field is short relative to some other process. In corrosion calculations, SKB considers several scenarios, with each scenario corresponding to different conditions in buffer and host rock, modelled as a series of diffusion legs. In release calculations, SKB considers series/parallel legs corresponding to different potential pathways to a flowing fracture.

SKB calculates time to steady state for release scenarios on the order of 30 years for nonsorbing species in a fracture and 50 R_{Nu} for nuclides in the buffer, where R_{Nu} is the nuclide retardation factor (TR-10-42, Section 7.2.1). SKB acknowledges that the Qeq approach is not valid and numerical methods are necessary for release of highly sorbing nuclides. We did not identify a description of the transient calculations during our review.

Corrosion processes involve nonsorbing dissolved species, thus time scales for reaching steady-state diffusion are less than 100 years, which is fast compared to changes in groundwater gradients and concentrations that evolve over glacial time scales. *We conclude that the steady state assumption is reasonable and appropriate for modelling (i) corrosion and (ii) release of nonsorbing to moderately sorbing radionuclides. We note that the steady state assumption may also apply to estimate peak release rates of highly sorbing radionuclides if they are sufficiently long-lived and waste-form degradation rates are slow relative to the steady-state criterion.*

It is typical in diffusion-controlled systems with a series of diffusion legs, for example transport of sulphide from a fracture to the copper overpack, that one of the legs controls total transport. This condition occurs because both concentration and flux must be continuous throughout the system. To illustrate the constraint applied by the continuity requirements, consider a one-dimensional system with two purely diffusive legs in series. Continuity in total flux at the transition from leg 1 to leg 2 requires that

$$Q = \left(\frac{DA}{L}\right)_1 (c_1 - c_i) = \left(\frac{DA}{L}\right)_2 (c_i - c_2)$$

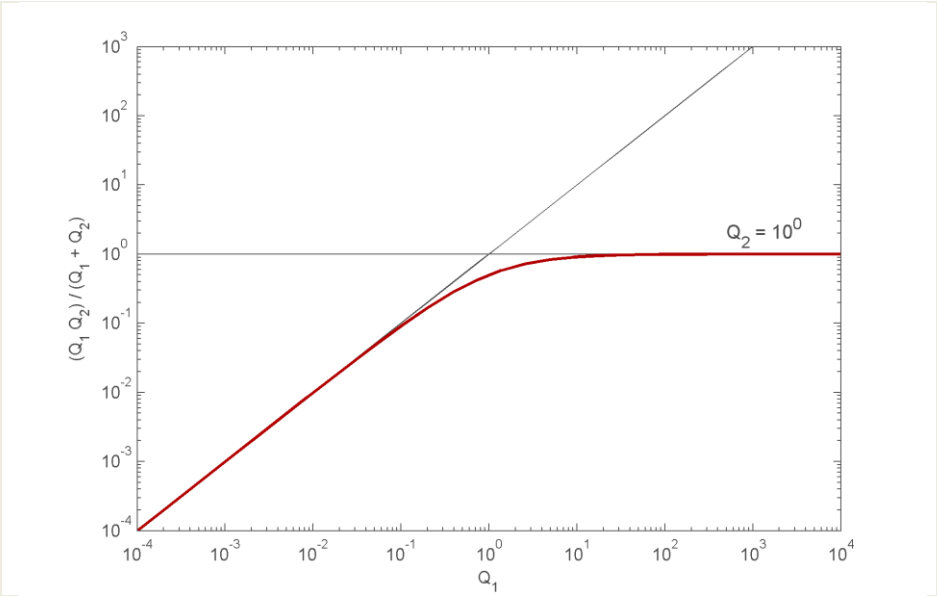

Figure 10: Inverse of effective Qeq formed by combining two legs in series, varying parameters for one leg and holding the other fixed.

where Q is total flux, D is the diffusion coefficient, A is the cross-sectional area for diffusion, L is the diffusion distance, c is concentration, and subscripts 1, 2, and i represent the upstream, downstream, and interface endpoints for diffusion.

In any particular diffusion leg, A/L depends on the corresponding geometry. SKB considers a variety of diffusion legs, such as a linear segment, radial diffusion from a pinhole, radial diffusion to and from a cylindrical segment, and diffusion within a boundary layer of water. SKB defines $DA/L = Q_{eq}$ for each diffusion leg. Making this replacement,

$$Q = Q_{eq1}(c_1 - c_i) = Q_{eq2}(c_i - c_2)$$

Eliminating c_i leads to the expressions

$$Q = \frac{Q_{eq1}Q_{eq2}}{Q_{eq1} + Q_{eq2}}(c_1 - c_2) = \left(\frac{1}{Q_{eq1}} + \frac{1}{Q_{eq2}}\right)^{-1}(c_1 - c_2) = Q_{ave}(c_1 - c_2)$$

$$c_i = \frac{Q_{eq1}c_1 + Q_{eq2}c_2}{Q_{eq1} + Q_{eq2}}$$

where Q_{ave} is half the harmonic mean of Q_{eq1} and Q_{eq2}. The smaller of the two Q_{eq} values is always within a factor of two of Q_{ave} (i.e., $Q_{min}/2 \leq Q_{eq} \leq Q_{min}$) and the larger value may differ substantially from Q_{ave}, as can be seen in Figure 10. By implication, a Q_{eq} value is not risk significant if it is more than an order of magnitude larger than the smallest Q_{eq} value, because transport is essentially unaffected by changes (uncertainty) in the larger parameter value.

The same approach for determining an overall Q_{eq} value for a series of diffusion legs can be applied in sequence when there are more than two legs in sequence: in this case, the smallest of the Q_{eq} values is always within a factor of N_{leg} of Q_{ave}, where N_{leg} is the number of legs. SKB typically uses two diffusion legs for

corrosion calculations, thus Q_{ave} is never more than a factor of two larger than the smaller of the two Q_{eq} values.

SKB considers branching near-field sequences in release calculations, with a two-leg diffusion pathway from inside the canister to the buffer and two or three parallel sequences (each with several legs) from the buffer to the far field (TR-10-50, Appendix G). Determining the risk-significant Q_{eq} value is more complex for release calculations, because total release is dominated by the parallel pathway with the largest release (hence largest constraining Q_{eq} value) rather than the pathway with the smallest constraining Q_{eq} value.

In SKB corrosion calculations, the copper canister end of the diffusion series has a zero concentration, reflecting instantaneous consumption of sulphide at the canister surface during copper oxidation. Accordingly, the rate of canister corrosion is linearly proportional to the far-field concentration. The background concentration may change over time, but at rates that are slow relative to the time to steady state in the near field. Corrosion rates determined for a particular Q_{eq} value and background concentration can simply be scaled by background concentration to take advantage of this linear dependence.

In SKB release calculations, the far-field end of the diffusion series has a zero concentration, reflecting diffusion into a reservoir with zero background dissolved radionuclides. Accordingly, the rate of release is linearly proportional to the concentration in the canister. For solubility limited radionuclides, the cap on the concentration difference from the canister to the far field implies that the limiting Q_{eq} value strongly constrains total release. When the radionuclide is not solubility limited, waste-form degradation determines total release and not the Q_{eq} value because concentrations within the canister adjust to whatever level is needed to drive diffusion at the degradation rate.

Risk-significant parameters

The SKB safety analysis asserts that the probability of any canister failing during the performance period is small. From a safety perspective, any potential increase in the probability of canister breaching is far more adverse than factors that affect release, because the description of release is immaterial unless a canister is breached. Accordingly, our assessment focused on factors that might increase the probability of canister breaching.

SKB stipulates that copper corrosion processes occur extremely slowly under nominal conditions (i.e., assuming an intact buffer), with canister penetration typically taking several orders of magnitude longer than the performance period. One assessment task was undertaken to probe and verify this important risk-significant conclusion that canister penetration rates are much longer than the performance period.

SKB considered a stylized buffer failure scenario to provide an indication of the consequences of a buffer failure. SKB considered buffer failure due to erosion for the analysis. SKB expects that groundwater conditions will change across a glacial cycle, such as fresh water recharging to repository depth under periglacial conditions, and sufficiently changed conditions could allow extensive chemical buffer erosion to occur. Sufficient buffer erosion allows water to contact the copper surface in greater quantities due to advective (rather than diffusive) conditions in the

buffer, thereby enhancing corrosion rates and subsequent release rates. SKB expects that sufficient erosion to adversely affect performance is highly unlikely, but performed a stylized analysis to assess the consequences should extensive erosion occur. The stylized buffer scenario requires extensive removal of buffer material, which SKB infers is highly unlikely because all deposition holes will be scanned for fractures prior to canister emplacement, and any deposition hole with a fracture sufficiently large to remove that much buffer material would not be used. A second assessment task in this review probed buffer erosion scenarios to assess whether the SKB-modeled hydraulic conditions at the set of deposition holes could preclude canister breaching under observed background sulphide concentrations even under the most pessimistic buffer conditions.

For completeness, a final assessment task examined release calculations to identify constraining parameters.

2.3.2. Confirmation of corrosion calculations

Metallic corrosion in an aqueous solution consists of two paired reactions, anodic dissolution of the metal (producing electrons) and cathodic reduction of oxidants in solution (consuming electrons). The metal dissolution rate is determined by the corrosion rate, which is controlled by the electrochemical balance between electron production and consumption rates in the anodic and cathodic reactions.

SKB considers two buffer scenarios for calculating canister degradation, the nominal scenario of an intact buffer and a hypothetic stylized calculation with an eroded buffer. SKB only considers corrosion for deposition holes contacted by a fracture. In the SKB calculations, sulphide from the background groundwater environment supplied to the copper canister surface balances copper dissolution at the rate of two moles of copper to one mole of supplied sulphide. SKB considers the copper shell to be the primary barrier isolating waste, despite the much greater thickness of underlying cast iron in the canister walls, because corrosion of the steel occurs at a much faster rate than copper corrosion under the expected environmental conditions. Copper canister breakthrough occurs when 5 cm of copper is dissolved at some location on the canister surface, completely penetrating the copper shell.

A safety case for an intact buffer can be demonstrated when the earliest breach that a canister experiences is long compared to the performance period even under the most adverse environmental condition expected at any deposition hole. Copper corrosion requires that an oxidizing agent such as sulphide migrate from the background environment to the canister surface. SKB considers that a flowing fracture contacting a deposition hole near the canister provides the readiest pathway for migration, and bounds the copper corrosion analysis with this scenario even though most of the deposition holes are unlikely to experience a noticeable fracture. *We agree that a fracture contacting the deposition hole provides a reasonable bounding analysis for copper corrosion.*

Illustration of SKB models of near-field transport for corrosion

SKB developed two primary models to analyze interactions with the environment, a nominal scenario and a scenario considering spallation of deposition hole wall. The nominal scenario considers a fracture that contacts an intact deposition hole perpendicular to the cylinder axis at the midpoint of the canister. This scenario considers flow in the fracture, with the flow velocity set to zero perpendicular to the

buffer at the edge of the deposition hole. For this scenario, sulphide is transported from the environment within the flowing fracture waters. A boundary layer of the flowing fracture adjacent to the deposition hole loses sulphide by diffusion to the buffer, which spreads from the fracture opening into the buffer and then diffuses within the buffer to the canister wall. SKB represents this as a two-leg pathway, with one leg consisting of diffusion within the fracture and the second leg consisting of radial expansion into the buffer from the circular trace of the fracture on the deposition hole wall. SKB also considers these two scenarios in radionuclide release calculations, with adding consideration of transport through the canister and alternate pathways.

SKB recognizes that the Qeq approach provides total sulphide mass flux into the deposition hole, not the local mass flux density along the canister surface that is relevant to corrosion, and recognizes that the mass flux density along the canister surface will vary with proximity to the fracture. Accordingly, SKB performed detailed numerical modelling to examine the spatial distribution of mass flux density along the canister surface, concluding that the peak flux density is seven times larger than would be calculated by dividing the total incoming flux by the canister surface area.

SKB also considers a scenario where the host rock adjacent to the deposition hole suffers thermal spalling along the length of the canister, allowing a permeable flow pathway along the deposition-hole boundary. SKB considers the nominal case more likely than the spalled scenario, because spalled rock resulting from construction will be removed prior to deposition and the waste loading strategy will limit the temperature change experienced at the deposition-hole wall. The permeable spalled zone allows water to focus towards the deposition hole, rather than diverting from the deposition hole, thus diffusion resistance in the fracture system is negligible. The amount of water focusing into the spalled zone is limited by the spatial extent of the fracture. SKB assumes that transfer of sulphide into the buffer occurs uniformly from the spalled zone, so that the average and peak mass flux density along the copper surface are the same (neglecting the surfaces at the canister end).
Figure 11 illustrates Qeq for both the fracture and the buffer, with and without spalling, using the model and nominal parameters described in TR-10-66. Three representative background hydraulic gradients are considered, roughly spanning the expected conditions at the site. SKB considers fractures with larger apertures likely to be detected in SKB's initial scan of the deposition-hole walls.

Figure 11 implies that the fracture system provides the constraining Qeq under essentially all conditions in the nominal scenario, but the buffer provides the constraining Qeq when background fracture flow is relatively large in the spalled zone scenario. The concentration at the deposition-hole wall is much less than the background concentration when the fracture system constrains Qeq, and is nearly at the background concentration when the buffer constrains.

The nominal and spalling scenarios differ largely because of the different flow patterns in the fracture. Flow diverges around the deposition hole in the nominal scenario. In contrast, the spalled zone induces convergent flow to the vicinity of the deposition wall because it is a high-permeability zone embedded in a low-permeability domain. Sulphide can only diffuse a limited distance as water passes by the deposition hole. By inducing convergent flow, a much larger volume of water passes within this critical distance. Note that these two conditions result in different signatures downstream of the deposition hole, with divergent flow resulting

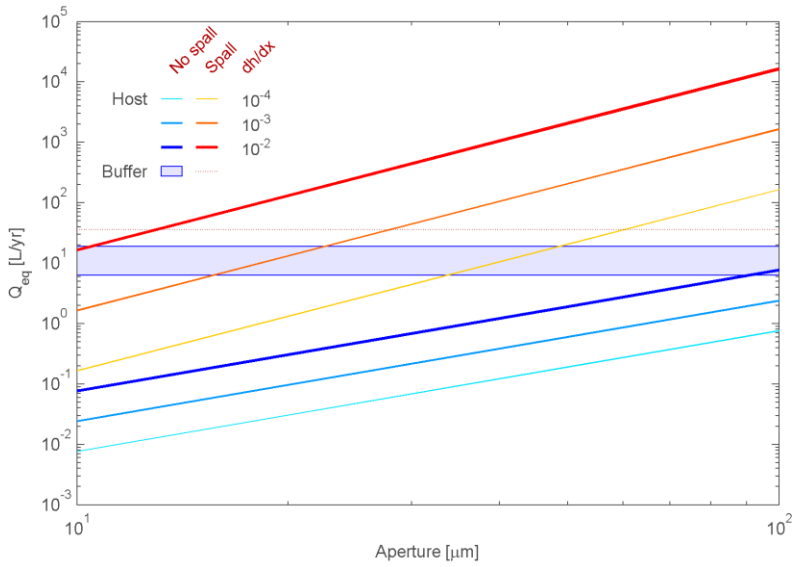

Figure 11: Effective Qeq for the fracture and buffer legs with representative fracture apertures and background hydraulic gradients, using SKB parameters and models.

in a thin trail of water with concentrations slightly above zero and convergent flow resulting in a wide swath of water with concentrations slightly below background.

We infer that the buffer is important in protecting against copper corrosion when there is convergent flow to the vicinity of the deposition hole.

Assessment of buffer defects on corrosion

SKB considers maximum canister corrosion rates with an intact buffer to be orders of magnitude slower than a rate that would cause canister breaching within the performance period. To better assess the roles of (i) the buffer and (ii) fracture position in copper shell corrosion, we independently developed several dozen exploratory 2D and 3D models of the near-field environment using the COMSOL Multiphysics model. These models considered a representative range of buffer and fracture characteristics. Some of the 3D models considered both flow and transport in discrete fractures that impinge on a buffer-filled deposition hole, with or without diffusive and advective defects in the deposition hole; others were limited to the interior of the deposition hole. This effort provided new appreciation for the computational efficiency of a network model relative to solving partial differential equations, especially for 3D models with fine features, as well as new appreciation for the COMSOL capabilities. These models informed our insights into the relative effects of diffusive and advective transport and the importance of flow convergence and divergence with respect to transport.

TR-10-66 assessed the potential for breaching the copper shell from sulphide-induced corrosion using deposition-hole-specific calculations. SKB extracted the fracture and hydraulic properties for each deposition hole from a realization of a site-scale discrete-fracture model, using three different conceptualizations of fracture properties to generate a discrete fracture network. SKB analyzed the 30 percent of the deposition holes contacted by a fracture, first discarding the 10 percent of these holes with fractures sufficiently large that the pre-emplacement inspection would have disqualified them. SKB concluded that an intact buffer

would preclude breaching of the copper shell, with maximum penetration depths of 0.06 and 0.6 mm in one million years for the no-spalling and spalling cases, respectively (TR-10-66, section 5.3.4). This corresponds to initial breach in 830 and 83 million years, respectively. SKB also considered a scenario with a partially eroded buffer for the same discrete fracture networks, assuming a stylized geometry to describe the eroded volume. The presented calculations indicate that the shortest copper shell corrosion time with a background sulphide concentration of 10^{-5} mol/L would be approximately 0.9 million years.

We interpret the presented information as suggesting that an intact buffer is important for limiting sulphide transport from the natural system to the copper shell by eliminating the effects of advection within the deposition hole.

SKB also provided calculations suggesting that, with an intact buffer, the fracture system provides the dominant resistance in the no-spalling scenario and the buffer reduces resistance by at most a factor of two for a few holes in the spalling scenario. We note that SKB considered three different correlation structures for the discrete fracture network, and used the correlation structure generating the slowest corrosion to perform this comparison.

We interpret the presented information as indicating that an intact buffer is important for constraining corrosion rates under only conditions with large convergent flows to the deposition hole.

Given the large margin between a risk significant penetration time and the performance period, our strategy for evaluating the risk significance of the Qeq approach is to identify scenarios with features that can cause much earlier penetration times than SKB identified. We use bounding assumptions for this purpose. We separately assessed the role of diffusion and advection within the deposition hole.

We first considered the portion of Qeq attributable to buffer diffusion resistance. This leg represents the engineered portion of the system, and its characteristics are less uncertain than the natural system. Our strategy is to provide a bounding calculation comparable to the SKB calculations, assuming that the fracture system does not contribute any barrier function. This provides a test of both the SKB Qeq calculations and the SKB safety conclusions derived from the Qeq calculations regarding penetration times due to corrosion.

The independent assessment uses a two-dimensional model in radial coordinates to represent the domain between the canister and deposition-hole wall, as shown in Figure 12. The canister and deposition hole are assigned the nominal SKB dimensions. The surface of the canister is assigned a zero concentration to represent complete sulphide consumption in copper corrosion. No mass crosses the top and bottom of the deposition hole, and no mass crosses the side wall except at a sulphide source. Two different diffusion coefficients are used, 10^{-9} and 10^{-10} m^2/s, to represent water and buffer materials, respectively. These values are comparable to SKB values.

The independent assessment assumes that the fracture system supplies an unlimited amount of sulphide to the deposition-hole wall at a concentration of 10^{-5} mol/L, which TR-10-66, section 4.3.5, describes as the 90th percentile of the distribution of observed concentrations). This concentration is less than the maximum observed value ($1.2 \cdot 10^{-4}$ mol/L, which is an outlier observation, an order of magnitude larger

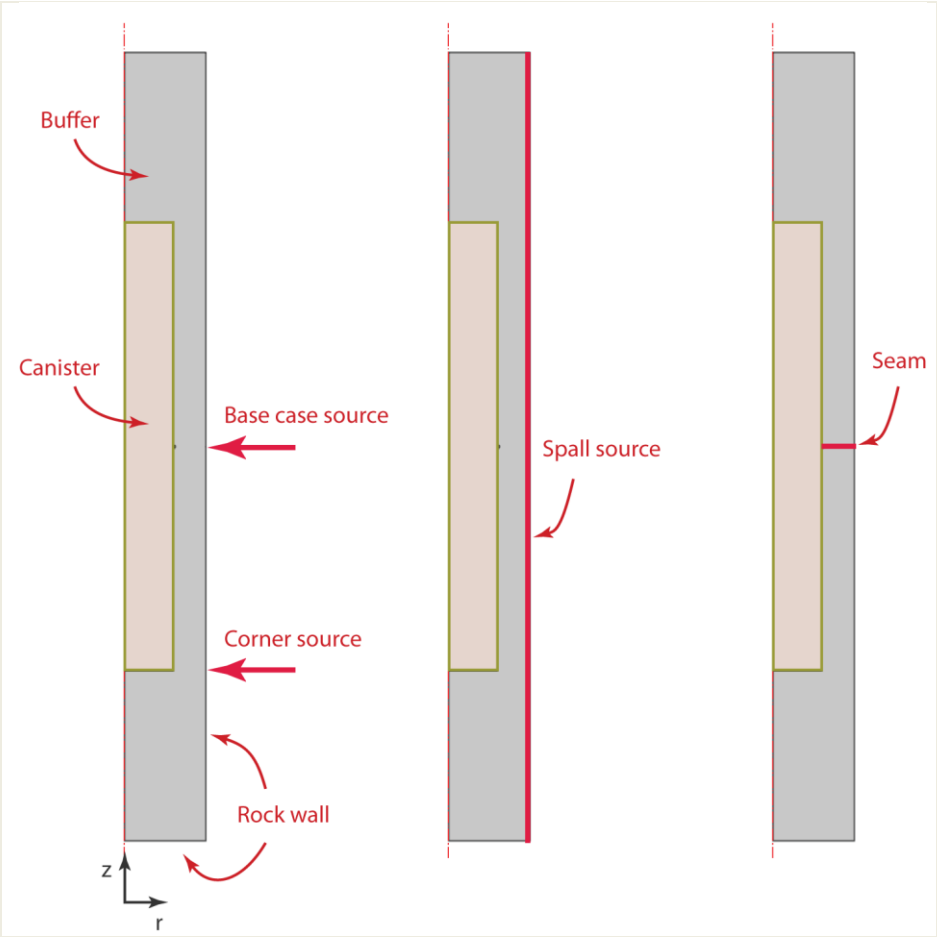

Figure 12: Schematic description of 2D radial model geometry for the deposition hole and canister, including source location scenarios.

than the next largest observed concentration). The assumption of unlimited supply may be unrealistic unless flow convergence occurs, based on Figure 11; if the fracture system limits sulphide supply, then actual corrosion rates would be smaller. Note that flow convergence may occur even without a spalled zone, for example if a pipe in the buffer develops immediately adjacent to a flowing fracture.

The assessment considers five distinct scenarios. The "intact" scenario assumes that there is a sulphide source 1 mm high (i.e., a 1-mm-aperture fracture) along the deposition-hole wall at the center of the canister and the "corner" scenario assumes that the same fracture is located at the elevation of the canister bottom. These scenarios bound the effects of fracture position. The "spall" scenario assumes that the entire deposition side wall is the source, representing an upper bound scenario for the source area.

The assessment considers two buffer defect scenarios, a global defect ("no buffer") and a local defect ("1 mm seam"). In both cases, the defect is assumed to contain stagnant water occupying a fraction of the deposition hole. The sulphide source is the same as the intact scenario for both defect scenarios. In the no-buffer scenario, the entire deposition hole is assigned stagnant water; in the 1-mm-seam scenario, a small seam between bentonite-buffer disks, and aligned with the fracture, is assumed to somehow have been formed and maintained despite the swelling capacity of the buffer.

Diffusion from a fracture source in essentially stagnant water may be a reasonable representation of sulphide transport within the deposition hole in the absence of a buffer, because (i) the exchange of water via fractures (even with flow convergence) is likely to be very slow compared to the storage volume within the deposition hole and (ii) flow in any spalled zone would be very small because of the hydrostatic pressure distribution in the adjacent deposition hole.

Figure 13a illustrates the initial copper corrosion rate along the copper canister, centered on the location of the peak corrosion rate. Peak (circles) and average (bars) rates for each scenario are summarized on the right axis. The peak corrosion rate occurs at the corner for both the corner and the spall scenarios, with the spall and corner lines truncated at the canister axis in Figure 13. For the other sources, the peak corrosion rate occurs at the midpoint of the canister. A modest peak does occur at the canister midpoint in the spall scenario. Comparing corrosion rates from the fracture scenarios and the spall scenario, fracture placement and uncertainty regarding spalling affect instantaneous buffer corrosion by roughly a factor of five. Comparing the two buffer-defect scenarios to the other scenarios, defects may increase the initial corrosion rate by roughly an order of magnitude (i.e., the ratio of diffusion coefficients). Interestingly, removing the buffer in a localized defect causes faster initial corrosion than removing the entire buffer. The buffer reduces lateral diffusion and allows a greater fraction of the diffusing sulphide to reach the canister. The size of the defect influences whether lateral diffusion out of the defect overwhelms preferential diffusion along the defect.

Figure 13b illustrates the breakthrough time at the average initial corrosion rate for each grid cell on the boundary. The initial corrosion rate is misleadingly slow when there is convergent diffusion to a corner (the corner and spall scenarios), because the total mass flux to the corner area is applied over a decreasing surface area as the corner is removed. The initial corrosion rate is misleadingly fast when the source is highly localized at the copper surface (the 1-mm-seam scenario), because a local source will create a divergent diffusion pattern that applies the same total mass flux to an increasing surface area as dissolution progresses. The circles in Figure 13b are an approximate estimate of the fastest penetration time that account for these radial effects, representing a removed area divided by the total flux contacting the canister within the area. For divergent diffusion, the area is half of a circle with a radius identical to the canister wall thickness (5 cm). For convergent diffusion to a corner, the area is a quarter of a circle with radius of $5\sqrt{2}$ cm, representing the distance from the exterior corner of the canister to the interior corner of the canister.

Figure 14 provides the diffusive flux magnitude and streamlines for the lower portion of the canister and deposition hole. The highest flux magnitude is located at the corner of the canister, illustrating the effects of convergent flow towards a corner. The effects are larger for a fracture located on the wall near the canister corner. For comparison, Figure 15 illustrates how a hypothetical localized source with a fixed concentration, analogous to a seam contacting the canister wall, will tend to develop a radially symmetric diverging pattern when the canister wall has a fixed zero concentration. Consumption from the localized source is dominated by the part of the wall nearest to the source, thus deep slits will tend to widen and wide zones will tend to deepen until the corroding segment of the wall is equidistant from the source.

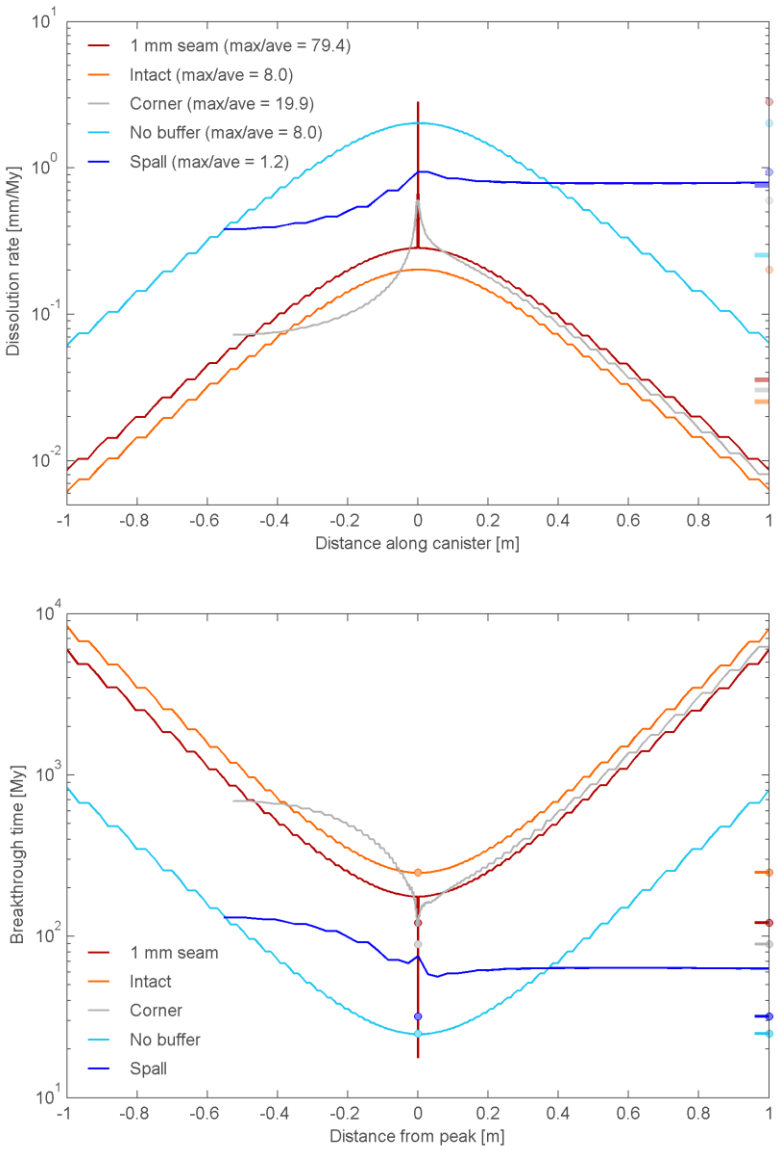

Figure 13: Spatial distribution, relative to the peak location, of (a) instantaneous corrosion rate and (b) corresponding time to penetrate a 5-cm copper thickness given a 10^{-5} mol/L sulphide background concentration. Symbols on right axis of (a) indicate peaks (circles) and averages across the entire canister surface (bars). Circles in (b) indicate average corrosion rate, correcting for radial diffusion at corners and seam endpoint.

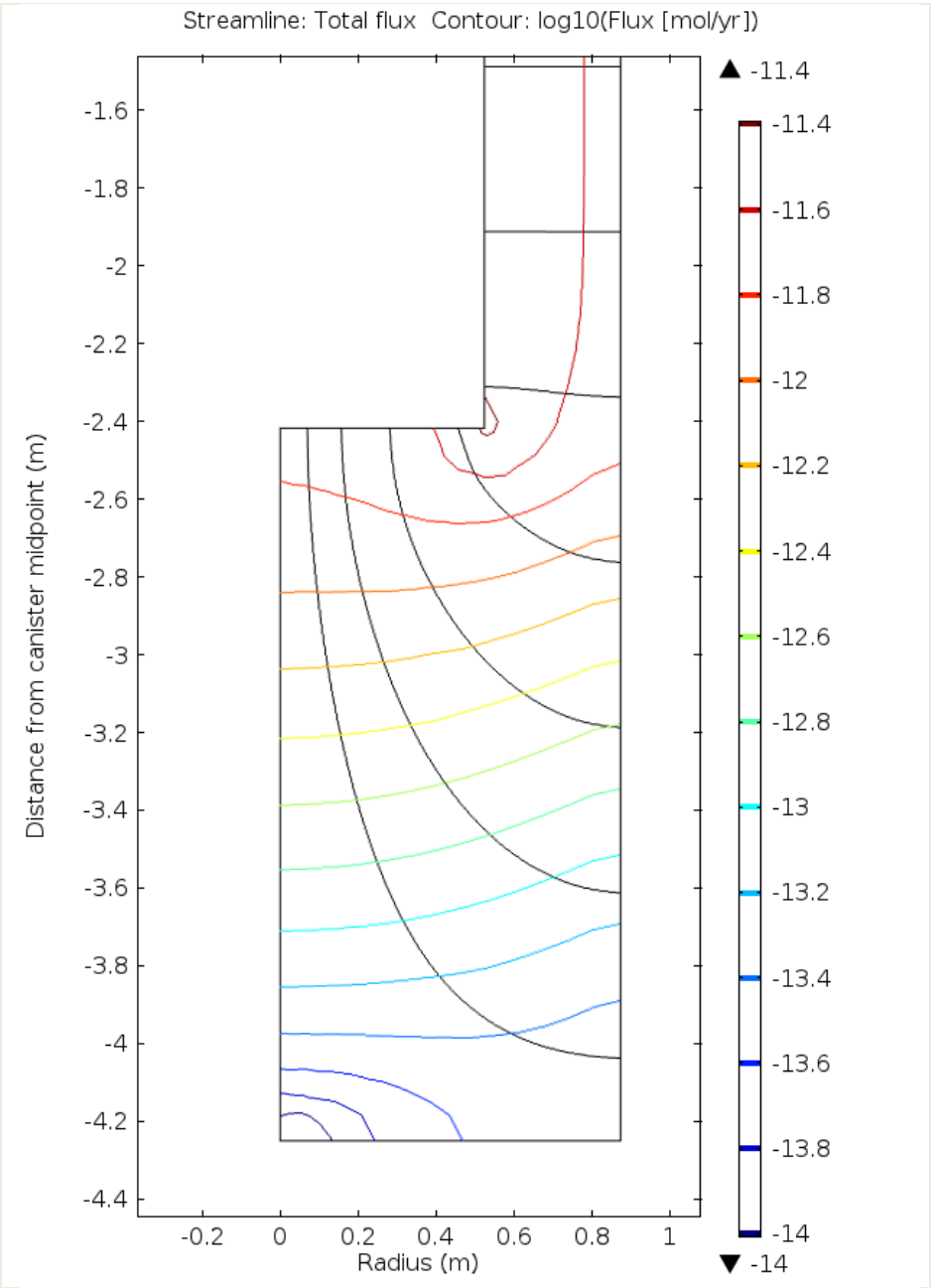

Figure 14: Streamlines and flux magnitude contours in the lower canister and deposition hole for the spalled source scenario illustrating radially convergent flow to the canister corner.

All of the considered cases have an initial breakthrough time between 25 and 250 million years, compared to a performance period of 1 million years. The corner scenario with a diffusion coefficient of pure water rather than buffer, which would have an initial breakthrough time of approximately 5 million years, is arguably the bounding case under diffusion-controlled conditions. With an intact buffer, corner corrosion with a spalled zone, with breakthrough on the order of 30 million years, provides a reasonable bounding case.

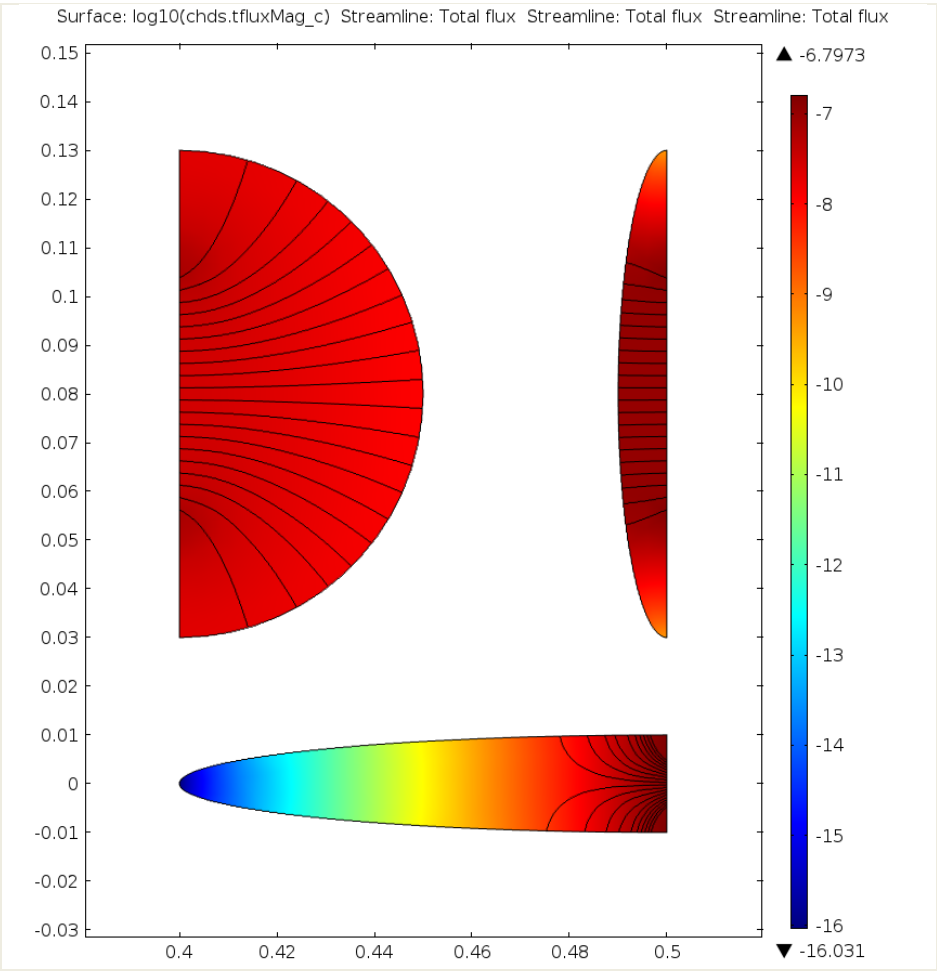

Figure 15: Streamlines and flux magnitudes for diffusion from a hypothetical source half the width of an opening, illustrating how radially divergent flow would develop given a localized defect. The colour scale represents the base-10 logarithm of the magnitude of diffusive flux.

The considered scenarios represent worst-case estimates for breakthrough time with stagnant conditions in the deposition hole given the assumed background concentration, because the fracture system may not be able to supply sufficient sulphide to maintain the calculated corrosion rates. Convergent flow to the deposition hole due to spalling or some gap next to the fracture is likely to be necessary to supply the assumed sulphide to the deposition hole with the assumed background concentration.

These calculated worst-case estimates are proportional to the background concentration, and increasing the background concentration would proportionately decrease the breakthrough time. Increasing the representative long-term-average background concentration by a factor of five would be necessary to decrease the breakthrough time to less than the performance period for the most adverse scenario considered (which is a nonphysical scenario). Increasing the representative long-term-average background concentration by a factor of 30 would be necessary to decrease the breakthrough time to less than the performance period for the most adverse physical scenario considered (corner corrosion with a spalled zone but intact buffer). The maximum observed concentration is only one order of magnitude larger than used in the assessment modelling.

We conclude that it is extremely unlikely that penetration of the copper shell will occur due to corrosion within one million years due to sulphide contacting the canister if conditions limit transport to diffusion within the deposition hole. This condition would require a combination of (i) time-averaged background sulphide concentrations experienced at the deposition hole during the performance period are larger than have been observed at the site to date, (ii) convergent flow to the deposition hole, and (ii) site conditions supporting significant flow to the deposition hole.

2.3.3. Advection-dominated corrosion calculations

TR-10-66 assesses the impact of partial buffer loss using a stylized corrosion calculation. In this analysis, SKB assumes that some combination of groundwater chemistry and fast flow has somehow been successful in partially eroding the buffer on one side of the canister into a roughly semicircular shape. SKB estimates that the height of the contact zone might range from 0.08 to 0.7 m, implying a total exposed copper area of 0.13 to 1.1 m^2 and void space in the buffer between roughly 0.06 to 0.54 m^3. SKB assumes that the removed volume is carried away in the fracture system. For assessment purposes, SKB assumes that the height of the contact area is equal to the thickness of the buffer and discounts diffusion into the buffer. The TR-10-66 rationale for the contact area is based on the dimensions of the assumed void. The SKB estimates of Qeq for the eroded buffer scenario are independent of the exposed contact area, thus the calculated corrosion rates are inversely proportional to the contact area.

TR-10-66 presented calculation results for canisters failing within one million years suggesting that buffer erosion times are unlikely to be significantly less than 100,000 year and corrosion penetration times are unlikely to be significantly less than 900,000 year with a background sulphide concentration of 10^{-5} mol/L and a corrosion zone height of 0.35 m. Changing the height of the corrosion zone to the lower-bound estimate of 0.08 m implies that the minimum corrosion penetration times would be approximately 200,000 years with the same background concentration. *We conclude that the contact area over which advective flow contacts the copper canister is a risk-significant parameter.*

In considering the consequences of buffer erosion, we considered how the physical scenario of a buffer erosion event might come about. Excavation of a void space in bentonite implies that surrounding bentonite would expand into the excavation. This expansion implies that a larger fraction of the bentonite mass would be removed from the deposition hole than implied by the fraction of the buffer space occupied by the void, creating a loss of density in the remaining buffer. This also implies that a continual erosion process would be necessary to counteract bentonite swelling unless sufficient excess pressure is maintained or the bentonite surface is sealed to prevent exchange of water. As the void grows, the water velocity in the void would tend to drop, yet buffer erosion would occur over a larger surface area. These processes tend to be self-limiting with respect to the maximum growth of a void space, and a large void may not be sustainable given the constraints offered by the natural system. Further, the SKB model suggests that a small contact area is risk significant.

Given these concerns, we considered what scenario might be consistent with site conditions that also provides a small corrosion area associated with advective flow.

Bounding conceptual model for pipe corrosion

In laboratory experiments, pipes have been observed forming along cylinder walls during bentonite rewetting experiments with constant applied flow rates (R-10-70). In the experiments, bentonite removal rates drop rapidly with time as the pipe develops but colloidal removal arguably continues at low rates for long periods. Observed pipes are associated with soft gel during the swelling process (TR-10-74, Section 3.3.4). The fact that pipes were observed forming in a bentonite experiment suggests a conceptual model for advection-dominated corrosion that operates with much smaller contact areas than considered in the SKB buffer erosion model.

The bounding conceptual model assumes that a small pipe consistent with the local hydraulic conditions has somehow formed in a way that it contacts the copper canister and persists in place for an indefinite duration. The excavated volume for such a pipe would be orders of magnitude smaller than the eroded buffer in the SKB concept, thus presumably such pipe could develop its final configuration much earlier after closure than the large void considered by SKB. Admittedly, it is not at all clear how a pipe contacting the canister might have formed in the first place. Piping in bentonite requires that (i) the water pressure in the pipe remains large enough to withstand the swelling pressure for a very long period, (ii) the hydraulic conductivity of the bentonite or a coating on the pipe walls is small enough to minimize water losses from the pipe to the buffer, and (iii) the water must be able remove eroded materials from the buffer (TR-10-74, Section 3.3.4). By implication, the fracture system must also be able to remove eroded buffer material from the vicinity of the buffer.

We expect that a pipe in a deposition hole is most likely to form between the buffer and deposition-hole wall along a fracture trace, because a small pipe would represent a flow-focusing mechanism that captures additional flow as the pipe increases in size. A pipe also might be able to develop from flow in a continuous initial gap between bentonite disks, for example. Perhaps an initially curving pipe running along the canister wall could slowly migrate across the buffer by preferential erosion on the inner face and preferential bentonite expansion on the outer face, thereby straightening until contacting the canister. Pipes along walls are favoured, because a given pipe area requires less buffer erosion to maintain itself, so a pipe contacting the canister would tend to remain against the canister but special circumstances would be necessary to detach a pipe from the deposition-hole wall. Regardless of the pipe-forming mechanism, we expect that the size of the pipe would be controlled by the interplay between available hydraulic gradient, capture zone area, pipe velocity, velocity-dependent erosion rate, and buffer swelling.

Our idea in considering corrosion as a result of the pipe is to identify whether corrosion rates under such an adverse scenario could be large enough to cause concern given the hydraulic and geochemical constraints offered by the natural system. We expect that it would be a strong argument for the safety of the proposed repository if such an adverse scenario could be eliminated. On the other hand, it would be important to consider in more detail how a pipe might be formed if the natural system could support a pipe at many of the deposition holes.

Representative hydraulic characteristics in the host rock

Flux-related near-field conditions important for estimating corrosion of a canister in a deposition hole include

- Presence or absence of a fracture intersecting the deposition hole
- Position of an intersecting fracture
- Flow rates in an intersecting fracture

The fracture network determines whether a fracture intersects a deposition hole and the position where it intersects. For fractures that intersect a deposition hole, the flow rates depend on local fracture apertures, global connectivity, and background hydraulic gradient.

SKB uses CONNECTFLOW to perform discrete fracture modelling. Fractures down to 0.4 m radius are included in the DFN flow model close to the repository, with large fractures tessellated to 10 m length (SKB R-09-20 p. 58 and 62). The equivalent continuous porous medium (ECPM) model has a 20 m element size in the local domain (R-09-20 p. 52), but the deposition hole has a radius of 0.875 m and the canister has a height of 4.835 m. Accordingly, ECPM model estimates must be scaled to the dimensions relevant to a deposition hole.

SKB (SSM2011-2426-130) provided a spreadsheet containing a base realization of the flow characteristics at 6916 modelled deposition holes, in terms of the main fracture intersecting the deposition hole. The worksheet with model outputs contains numerous tersely labelled columns, without an explanatory key or units for each column. These columns appear to be described in R-09-20 (Appendix B). Separate worksheets provide interpreted and fully labelled columns providing (either directly or by backtracking worksheet calculations) estimates of (i) volumetric flux per unit fracture width, (ii) fracture aperture, and (iii) average velocity. These estimates appear to represent average values perpendicular to the flow direction. Most (60 percent) of the holes had no intersecting fracture or zero modelled flow. Figure 16a indicates the modelled fracture-average volumetric fluxes and apertures and Figure 16b indicates estimated hydraulic gradients. Hydraulic gradients are estimated assuming that $T = (2b)^2$, where T is transmissivity and b is the fracture aperture (Equation 4-6 in SSM2011-2426-130). The symbol for each deposition hole is drawn the same way in both parts of Figure 16.

SKB intends to discard deposition holes with a large visible fracture, implying that the deposition holes with the 4.5 mm aperture shown in Figure 16 would not contain a canister.

TR-10-50 (Section 2.1.2) discusses the evolution of flow over a glacial cycle in response to climate change, including glaciations. The flow scaling factors presented in TR-10-50 (Figure 2-3) imply that the time-averaged flow during an entire glacial cycle is roughly 2.3 times the flow during the temperate period, with brief peak intervals in which flow may be 50 times the flow during the temperate period as an ice sheet retreats.

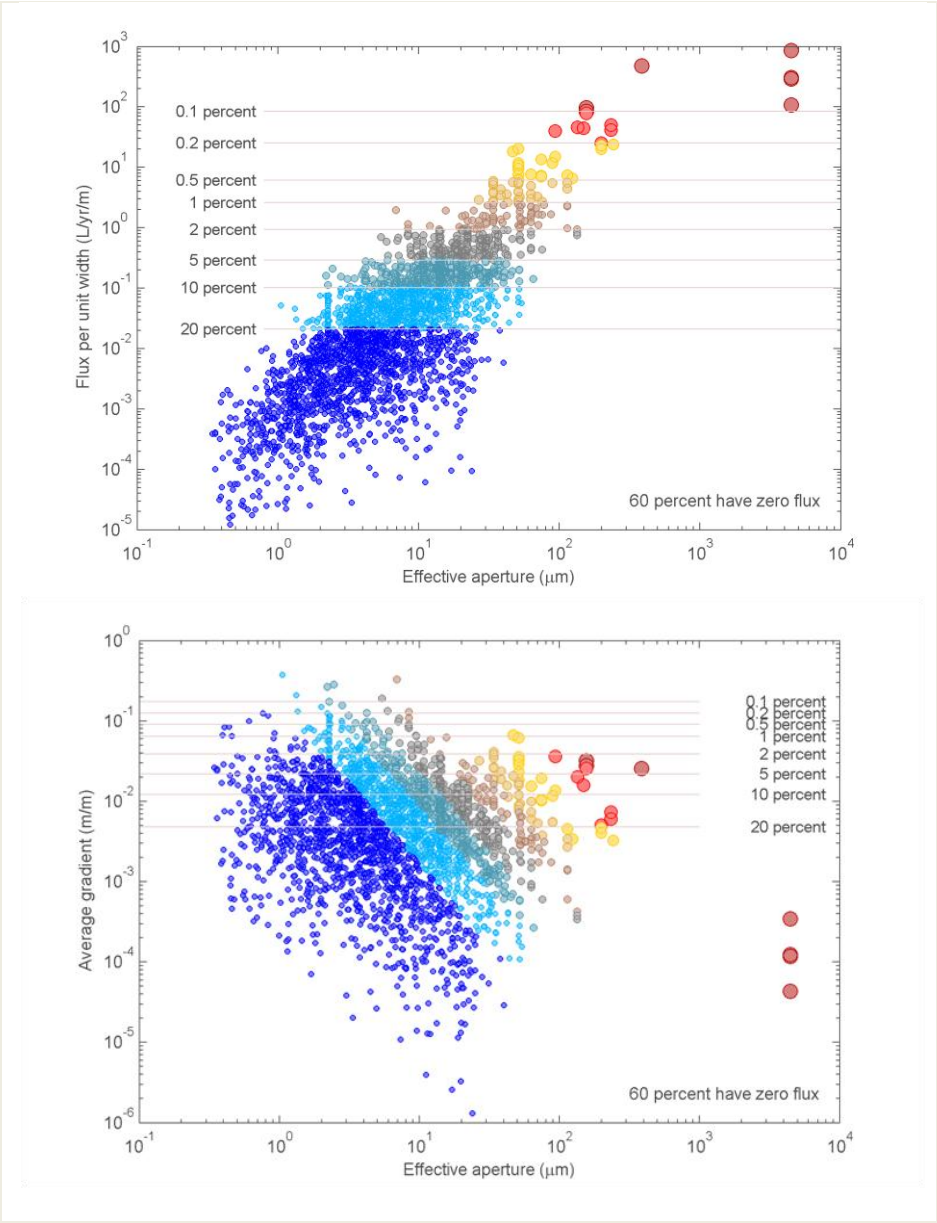

Figure 16: SKB base case realization r0 simulation results (SSM2011-2426-130 spreadsheet).

Pipes consistent with SKB hydraulic simulations

Without speculating on precisely how a pipe would form through a bentonite buffer and how the opening would maintain itself over long periods of time, an example illustrates that a pipe consistent with site hydrological conditions might allow greatly accelerated general corrosion rates on a small area of the canister.

Under laminar conditions, the average velocity of water in a pipe, v_{ave}, is

$$v_{ave} = \frac{\rho g r^2}{8\mu}\frac{dh}{dx}$$

where ρ is density, g is the acceleration due to gravity, r is the pipe radius, μ is viscosity, and dh/dx is the head gradient in the pipe. Total volumetric flux in the pipe is

$$Q = \pi r^2 v_{ave}$$

Combining,

$$Q = \frac{\pi \rho g}{8\mu} r^4 \frac{dh}{dx}$$

The pipe radius strongly influences both the flux through the pipe and the velocity within the pipe.

The flow through a pipe is constrained by the hydraulic conditions in the surrounding fracture system. Assuming that a single pipe intercepts flow, an approximate upper bound on pipe flow might be the amount of flow intercepted by half the diameter of the deposition hole, with the remainder diverting laterally around the deposition hole. Similarly, the surrounding fracture system constrains the hydraulic gradient in the pipe not to be much larger than the background hydraulic gradient. A smaller hydraulic gradient would imply that some funnelling into the pipe is occurring, with the degree of funnelling constrained by the velocity required for the erosion necessary to maintain an open pipe in the face of bentonite swelling.

Assuming that the worst case scenario is the upper bound pipe flux, the minimum pipe radius is

$$r_{min} = \left[\frac{Q_{max}}{(dh/dx)_{bg}} \frac{8\mu}{\pi \rho g} \right]^{1/4}$$

The maximum average velocity through the pipe occurs with the minimum radius, leading to

$$v_{max} = \frac{Q_{max}}{\pi r_{min}^2}$$

Figure 17 illustrates the distribution of calculated r_{min} and v_{max} values for the SKB r0 fracture fluxes and gradients at deposition holes shown in Figure 16, using the same colour coding as Figure 16. Two lines are drawn for each deposition hole to indicate bounds on how velocity might respond as the pipe radius increases, and thereby decreases the hydraulic gradient within the pipe that is necessary to carry a given flux. Both lines consider the consequences of reducing the gradient in the pipe by an order of magnitude relative to the background gradient. The slanted lines ignore the additional funnelling to the pipe that would occur, while the horizontal lines assume that reducing the pipe gradient induces a proportional increase in the background flow funnelled to the pipe. Given that the spacing between deposition holes is approximately 7 times the deposition-hole radius, an order of magnitude increase in flux funnelled to the pipe may be a reasonable upper bound.

The example is based on a 1-mm diameter pipe carrying flow of 1.6 L/yr at a background concentration of 10^{-5} mol/L. Assuming that all flow is captured in a width equal to the canister radius, this flow rate is exceeded at approximately

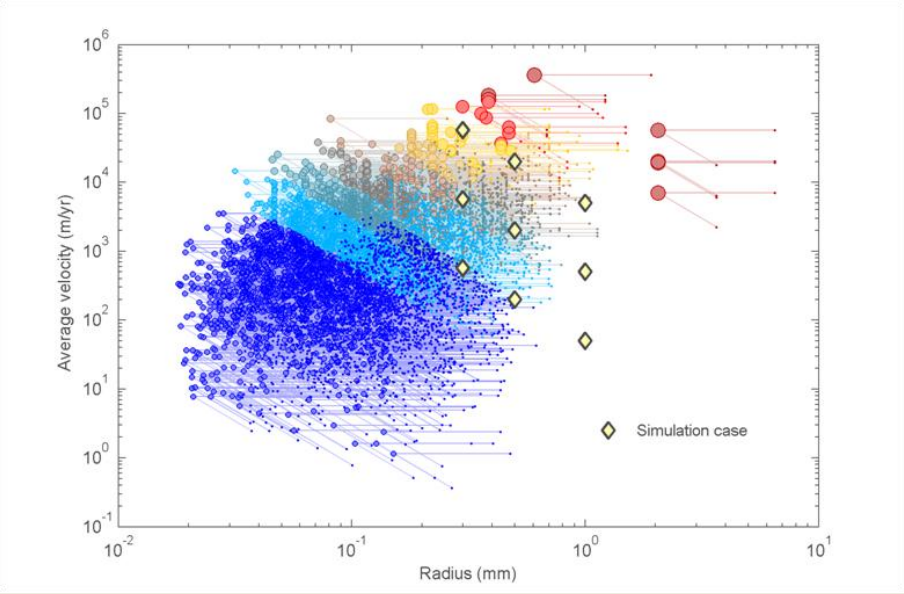

Figure 17: Scatter plot of limiting pipe radius and velocity given fracture fluxes and gradients at deposition holes in the SKB r0 realization. Symbols use colour scheme from Figure 16. Lines illustrate the consequence of reducing pipe gradient one order of magnitude relative to background with flux capture multiplied by 1 (slant) and 10 (horizontal).

1 percent of the deposition holes in SKB realization r0 (Figure 17). To examine sensitivity, three velocity scenarios (multiplying the base rate by 0.1, 1, and 10) and three pipe diameters (0.6, 1, and 2 mm) are considered. These nine cases are labelled "Simulation case" in Figure 17, with the nominal case in the middle. The nominal case is also considered with background concentrations that are multiples of the nominal background concentration.

Pipe-flow simulations

More than a dozen COMSOL models were constructed to consider a simplified representation of the system. Across all of the COMSOL models we considered, the highest corrosion rates consistently occurred where a pipe first contacts the copper. Because of the large contrast in scales between a small pipe and the canister and deposition hole, which causes substantial difficulty in gridding the system, we developed a scenario to capture the key aspects of the system with a relatively simple grid. The competition between advection and diffusion is a key factor in this system, because diffusion from the pipe to the buffer strongly dilutes pipe water concentrations when the pipe velocities are small.

The simplified system shown in Figure 18 considers (i) a straight cylindrical pipe with constant radius, (ii) a surrounding bentonite cylinder, and (iii) the outer edge of the canister essentially tangent to the pipe. The canister carves out part of the bentonite cylinder. The pipe and bentonite cylinders have the same length as the deposition-hole diameter. If the deposition hole geometry was considered, a curved section would be missing on both ends of the bentonite cylinder. The analytic velocity distribution within the cylindrical pipe is parabolic, assuming that flow is laminar and constant. The sulphide concentration is fixed at the background value at the inlet to the pipe, essentially assuming that diffusion within the fracture is overwhelmed by flow convergence. The copper canister and the outer edge of the

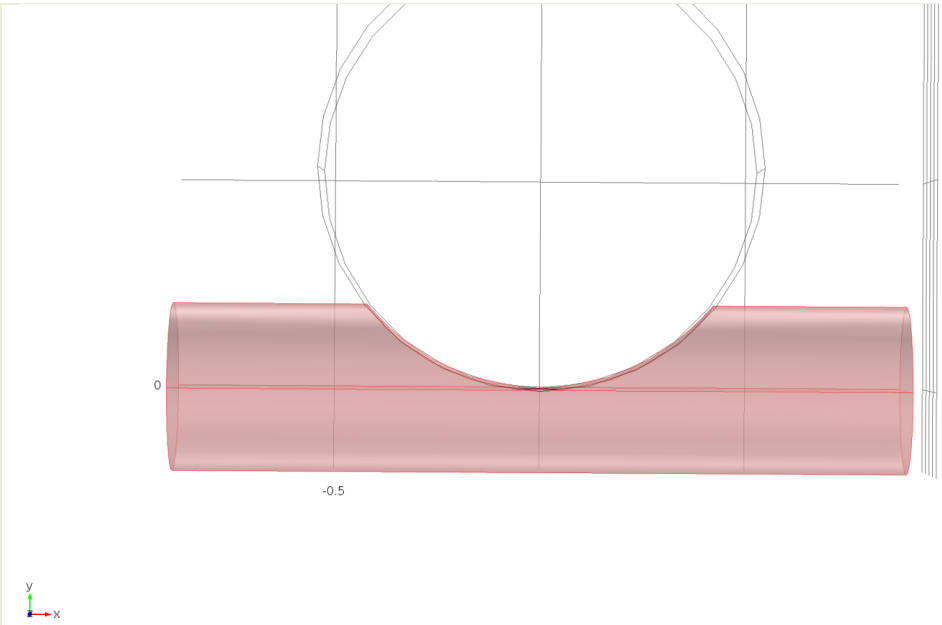

Figure 18: Geometry of the pipe simulation. The highlighted zone is the simulation domain, represents a bentonite cylinder cut by a canister. The pipe is located at the bentonite cylinder centre line. Deposition-hole boundaries are neglected at the ends of the simulation domain.

bentonite cylinder are assumed to have zero concentration, maximizing diffusion from the pipe.

To represent the scenario of a pipe glancing along the canister wall, which over time would cut a semi-circular groove into the copper, the pipe centreline passes 2 mm inside the outer boundary of the copper shell. To overcome gridding constraints, a cylindrical region with ten times the radius of the pipe surrounds the pipe, forming a groove in the copper shell where it overlaps. The half of the pipe facing the copper shell is assumed to have a zero-concentration boundary to represent contact with the copper.

Figure 19 illustrates the distribution of early dissolution rate along the copper surface for a nominal 1 mm diameter pipe scenario, with an average pipe velocity of 2000 m/yr and background sulphide concentration of 10^{-5} mol/L. The dissolution rate represents general corrosion, not pitting corrosion, even though the peak dissolution rate is highly localized. The peak dissolution rates occur in only a few square millimetres. If it were physically possible to maintain the peak dissolution rate on the same area, it would take approximately 61,000 years to breach the canister. However, the peak early dissolution rate (i.e., the upstream end of the exposed copper) is not representative of the evolution of the entire penetration. If transport is locally dominated by diffusion once dissolution becomes established, the local system would tend to evolve towards a roughly hemispherical dissolution surface. The dissolution surface will be somewhat elongated because of flow in the pipe, perhaps mediated by local buffer swelling as the dissolution front advances, but for order-of-magnitude estimation purposes it is reasonable to assume that the penetration evolves in a diffusion-controlled pattern.

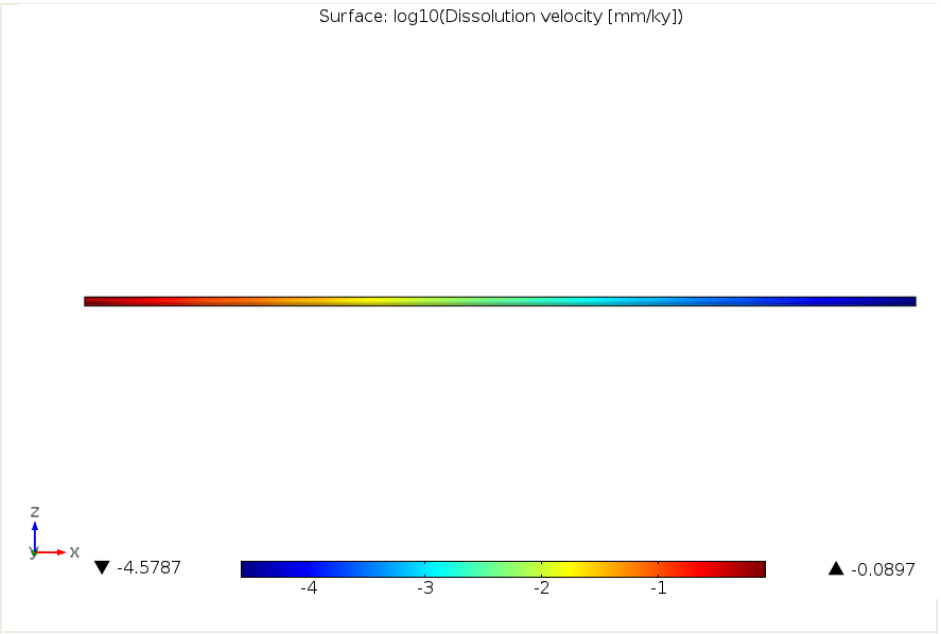

Figure 19: Rate of copper removal along the segment of 1-mm diameter pipe with a zero concentration boundary condition. Flow is from left to right. The local removal rate decreases exponentially from 0.81 to $2.6 \cdot 10^{-5}$ mm/ky over the 9.2 cm length of the exposed zone.

Penetration time

Given the highly concentrated uptake of sulphide at the copper surface resulting from pipe delivery, it is difficult to estimate penetration time for this case. It is clearly unreasonable that the peak delivery rate can be sustained on a single small area, because the required depth for penetration is at least an order of magnitude larger than the pipe diameter. Given a fixed pipe location, a small-radius divot at the initial area with peak delivery would take a hemispherical shape, because the corrosion rate inside the divot would be controlled by radial diffusion in stagnant water within the divot. Sufficient copper removal would leave a void space with locally slow velocities that are less capable of supporting bentonite erosion against continued bentonite swell, so presumably the pipe would migrate to follow corrosion of the copper surface. Flow in a small-diameter divot is energetically unfavourable, so the pipe would likely migrate laterally and spread around delivery to the copper surface. More detailed investigation would be necessary to resolve the likely behaviour; for bounding analyses we assume that the pipe migrates to deliver sulphide uniformly over the surface of an enlarging hemisphere.

Assuming that (i) the actual penetration excavates a spherical depression in the copper surface and (ii) the initial volumetric rate of copper removal Q (i.e., volume/time) as estimated by transfer from the pipe to the exposed copper remains constant, a shell balance can be integrated to estimate the time required for a hemisphere to increase to 5 cm radius. Half the surface area of a sphere with 5-cm radius is $1.57 \cdot 10^4$ mm^2, thus the final dissolution rate is roughly 4 orders of magnitude slower than initial peak dissolution rate.

The rate of expansion of a spherical shell with a constant molecular flux 2Q is

$$\frac{dr}{dt} = \frac{2Q}{A} = \frac{2Q}{4\pi r^2}$$

where r is the radius, t is time, and A is the area of the shell. Rearranging and integrating,

$$T = \int_0^T dt = \int_0^R \frac{2\pi r^2}{Q} dr = \frac{2\pi R^3}{3Q}$$

In this relationship, R is the thickness of the copper shell and T is time for first penetration. This provides a geometric scaling to translate the initial delivery of rate of sulphide from the pipe to the entire exposed copper surface into a penetration time.

Figure 20 illustrates sensitivity results for combinations of pipe diameter and velocity. The results are expressed as time for dissolution to penetrate 5 cm at (i) the initial peak dissolution rate and (ii) accounting for diffusion-limited growth of a hemispherical shell. The horizontal axis in Figure 20 is the incoming concentration times the volumetric flow rate in the pipe. In Figure 20, symbols labelled with c_0 represent simulation results using a background concentration of 10^{-5} mol/L and symbols labelled with $c_0/5$ or $c_0 \times 5$ are calculated by simply scaling the input flux and failure time.

The initial peak dissolution rate estimate is somewhat affected by gridding, but roughly scales with the inverse of the pipe diameter. This is consistent with the same total consumption spread over an area proportional to the pipe diameter. The different pipe diameters result in similar total sulphide delivery to the copper surface, based on the similar time to penetration when the spherical integration is considered.

There is a clear transition from advection domination to diffusion domination as the pipe flux decreases, with very different responses to input flux. Diffusion domination occurs when pipe flux is below roughly 0.8 L/yr, left of the distinct break in the slope of peak initial dissolution rate. Advection domination occurs when pipe flux is above roughly 8 L/yr, marked by a flattening in the slope of peak initial dissolution rate. The sensitivity of the sphere penetration time to flux can be written as

$$\frac{T_2}{T_1} = \left(\frac{Q_1}{Q_2}\right)^{\alpha}$$

where Q is inflow rate and T is time to penetration. In the simulation results, the exponent α increases from 1 in the advection dominated regime to more than 7 in the diffusion dominated regime.

Consequences for canisters

The discrete fracture network results provide a framework for considering consequences of pipe flow for the repository system. For this purpose, the penetration-time response of the 1-mm diameter pipe with respect to pipe flow is reasonably consistent with the other pipe diameters, thus the tabulated values from the 1-mm pipe simulations can be used to interpolate for all of the pipes.

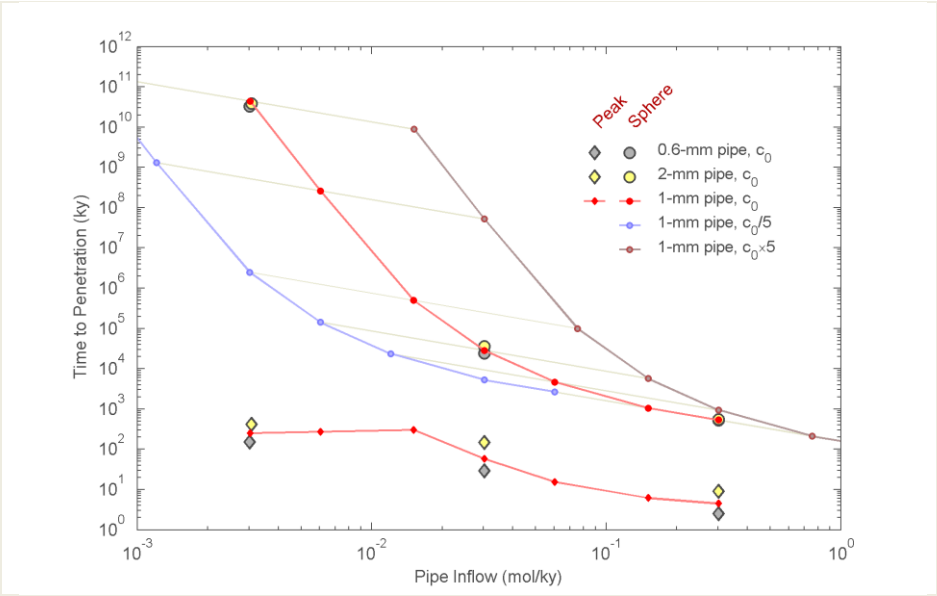

Figure 20: Time to penetrate 5 cm of copper given pipe supply of sulphide at the initial peak dissolution rate and accounting for diffusion-limited growth of a hemispherical shell.

Figure 21a illustrates the penetration time for a hemisphere dissolved for the pipes developed from the SKB realization r0 simulation (i.e., the pipes in Figure 17), using the same colour coding as Figure 16. The background concentration of sulphide entering the pipe is 10^{-5} mol/L; penetration time is inversely proportional to background concentration. The penetration time calculation assumes that all background sulphide is funnelled into the pipe (diffusion to the buffer within the fracture system is negligible). This assumption overestimates pipe delivery rates; in particular, a substantial amount may diffuse directly from the fracture to the buffer at low flow rates, similar to the intact-buffer scenario.

Figure 21b compares the time of penetration with pipe flow to the time of penetration for diffusion through an intact buffer for the same deposition hole (i.e., using the simulation results shown in Figure 13). The crossover between advection and buffer diffusion as the dominant behaviour occurs when the pipe has a flow rate of approximately 1 L/yr. However, the fracture system tends to be limiting at low flows for the diffusion-only case, implying that the crossover point would occur at even smaller flow rates.

Figure 21 suggests that pipe flow (if it occurred) would yield shorter penetration times than the nominal scenario for 5 to 10 percent of the deposition holes, or 350 to 700 canisters. However, even if every hole experienced the enhanced dissolution rates from pipe flow, only approximately 0.5 percent of the deposition holes (about 35 holes) would experience a penetration time shorter than the performance period of one million years, and SKB indicated that several of these holes would have been screened out by visual inspection prior to canister emplacement. We expect that pipes are most likely to form under the relatively high-flow conditions that are associated with fast corrosion.

2.3.4. Release calculations

We performed a much more limited assessment of the SKB transport release approach relative to our assessment of the SKB corrosion calculations, because a

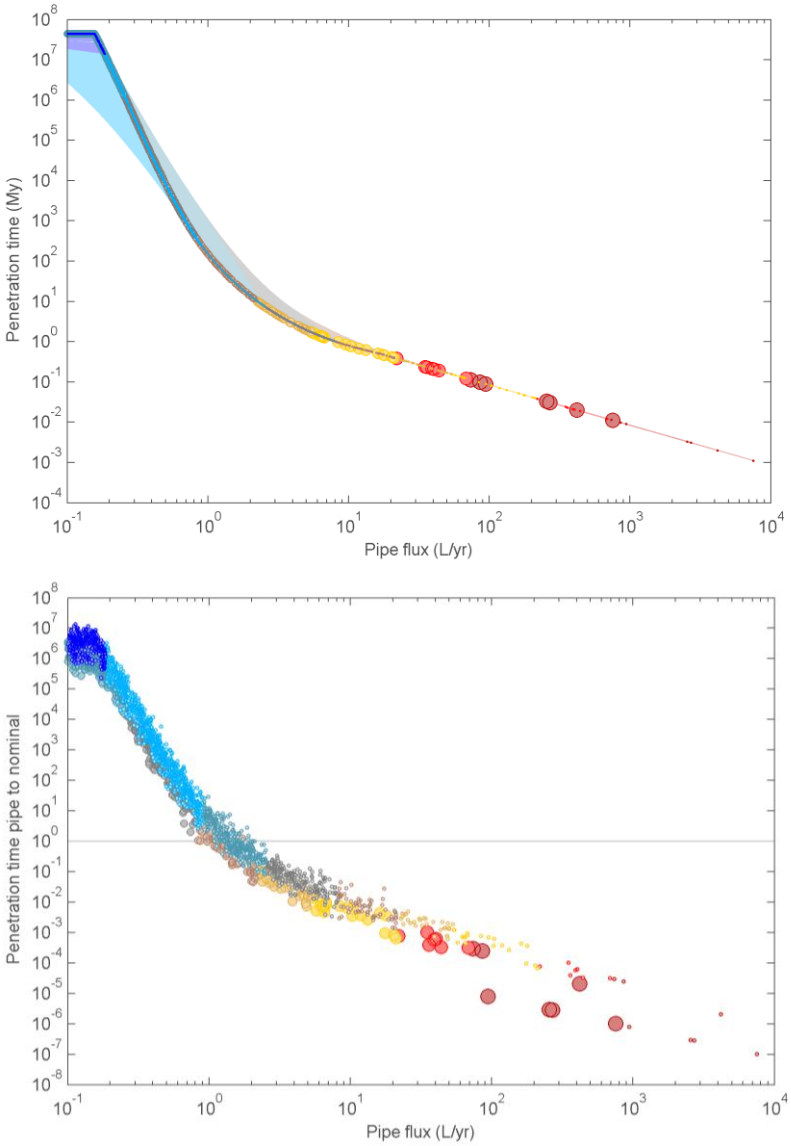

Figure 21: Estimated penetration time as a function of volumetric flux in the pipe for (a) spherical dissolution at the pipe/copper contact and (b) ratio of penetration times for pipe flow relative to the nominal intact-buffer scenario (see Figure 13), using the set of pipes illustrated in Figure 14.

potential for additional failures through corrosion is more risk-significant than release from hypothetical scenarios.

We considered the release calculations in two ways: (i) a high-level assessment of the SKB hypothetical failure scenarios, focusing on consistency; and (ii) a high-level assessment of the potential consequences of the pipe-induced corrosion failure scenario considered in Section 2.3.3.

Assessment of hypothetical failure scenarios

The SKB safety case considers three hypothetical release modes: (i) release from a canister breach due to isostatic loading, (ii) release from an undetected pinhole failure in the canister, and (iii) release from a canister breached because of buffer erosion and subsequent corrosion. SKB considers these failure mechanisms to be hypothetical, because they are so unlikely that failure is unlikely to occur for even one canister in the repository.

SKB analyzes the hypothetical release scenarios by considering transport pathways from the canister to the environment, but the release scenarios have somewhat different pathways. Failure and release are decoupled in the isostatic loading and pinhole scenarios, but in the eroded-buffer scenario both failure and release are tied to water flowing through the eroded portion of the buffer.

The buffer remains intact in SKB's isostatic loading and pinhole defect scenarios. SKB considers three release pathways: (i) release to a fracture contacting the buffer (Q1 pathway), (ii) release to the excavation damaged zone (EDZ) surrounding the overlying tunnel (Q2 pathway), and (iii) release to water flowing within the head space of the tunnel itself (Q3 pathway). The Q1 pathway is only active for the subset of deposition holes with a fracture contacting the deposition-hole wall. The Q2 and Q3 pathways are always active.
In the SKB release model, the pinhole is described as a 2-mm cylinder active for 10^4 years. During this period, the pinhole radius is so small that it dominates overall Qeq (Qeq for the cylinder is $8 \cdot 10^{-4}$ L/yr and Qeq for the expansion from the pinhole to the buffer is 0.04 L/yr, compared to other legs that have a minimum Qeq of 0.1 L/yr). After 10^4 years, the pinhole is assumed to fail, and the waste is released to the buffer in a zone that is 0.5 m in height (the canister essentially loses its resistance to release). After failure, the overall Qeq is dominated by Qeq for transport from the buffer to a flowing fracture in the natural system. The isostatic loading scenario assumes that the canister remains intact for 10^4 years, then waste is free to contact the buffer.

Erosion of the buffer allows sulphide to contact the canister wall and breach the canister in the eroded-buffer scenario. SKB represents this case by allowing releases to move directly from the canister into the water flowing within the eroded buffer.

We performed a much more limited assessment of the SKB transport release approach relative to our assessment of the SKB corrosion calculations, because a potential for additional failures through corrosion is more risk-significant than release from hypothetical scenarios.

We confirmed that SKB's overall methodology for calculating releases is consistent with SKB's overall methodology for calculating transport of sulphide to the canister surface.
We confirmed that the input parameters used for the analyses were consistent between release and corrosion calculations.

We examined the implementation of the near-field transport model in some detail. TR-10-50 (Appendix G.2) describes the near-field release calculations using COMP23 in a manner that implies that the formulation may be inconsistently implemented. As described in Section 2.1.4, COMP23 considers three radionuclide

release pathways (Q1, Q2, and Q3). TR-10-50 (Appendix G.2) describes each pathway as having an equivalent resistance obtained by summing the resistances of several blocks. This representation would be correct if each release pathway was independent of the other pathways. However, the corresponding flow diagram (reproduced as Figure 9) implies that the diffusion network branches at two intermediate points: (i) where Q1 separates from Q2 and Q3, and (ii) where Q2 separates from Q3. For consistency, the concentration at the branch points must be equal for each pathway. This requirement is not enforced if COMP23 calculates releases by independently summing resistances in each pathway. Independently summing resistances results in overestimates of release by a factor of 1 to 3, depending on the set of resistances for each pathway.

We conclude that COMP23 may overestimate total release rates by as much as a factor of 3 if the algorithm is implemented according to the description. However, it is not clear whether the description in TR-10-50 (Appendix G) describes the actual algorithm or is meant as an illustration.

We performed limited 3D modelling using COMSOL to examine geometrical aspects of the pinhole failure scenario. In this modelling, the model domain consisted of the buffer inside the deposition hole (i.e., we did not consider the cylinder through the canister or transport in the fracture system). We considered two scenarios, (i) one or two fractures along the deposition-hole periphery with zero concentration and (ii) a fracture along the periphery with zero concentration coupled with an excavation damaged zone with flowing water at the top of the deposition hole. We found that

- Total flux through the system was proportional to the pinhole radius
- For a single fracture, total flux through the system was insensitive to fracture position or aperture
- Total flux through the system was insensitive to the number of release zones (fractures plus excavation damaged zone)

We concluded that the COMSOL model results considering the effects of geometric factors are consistent with SKB's analysis.

We considered SKB release scenario results (TR-11-01, Section 13.7; TR-10-50, Section 6.4) for consistency with the Qeq information presented by SKB. The pinhole scenario and the isostatic load failure scenario with a single failed canister (failure occurs at 10^4 years after closure) provided essentially identical far-field dose consequences after 10^4 years, consistent with presumably identical buffer to far-field Qeq values.

Releases for the pipe scenario

We developed a conceptual model for the release process under the pipe scenario, but did not perform detailed release calculations.

The pipe scenario assumes that a pipe remains open against the bentonite swelling pressure and presses against the canister wall until the copper shell breaches. During the corrosion process, the pipe migrates back and forth slightly so that the opening in the copper shell is roughly hemispherical. Once the shell is breached, water contacts the underlying steel and it begins to rapidly corrode. The steel corrosion products expand, pressing against the copper shell and widening the initial

breach. Ultimately, a conduit to the canister interior opens, allowing releases to the pipe. A large opening would permit bentonite to expand into the canister interior, displacing the pipe laterally.

In this scenario, we expect that the releases would be constrained by transport from the canister interior to the pipe. If no credit for resistance in the steel is taken, there is minimal resistance from the canister interior to the pipe. The consequences may be comparable to the pinhole scenario once the pinhole resistance becomes negligible (after 10^4 years in SKB analyses) for holes where the Q1 (fracture) pathway has a large Qeq. Given our assessment that approximately 0.5 percent of the deposition holes have hydraulic conditions that might induce breakthrough within one million years, only the largest Q1 pathways are relevant for release calculations in this scenario.

TR-10-50 (Figure 6-50) suggests that the peak and million-year release rates for the 99^{th} percentile Q1 pathway are approximately 2.5 and 0.13 μSv/yr, respectively, compared to the regulatory risk limit of 14 μSv/yr. Figure 6-50 implies that the peak rates occur over several tens of thousands of years and are roughly proportional to the flow rate in the Q1 pathway. On the other hand, the million-year release rates appear to be much less affected by the Q1 pathway flow rate.

Given these observations and assuming that every canister experiences the 99^{th} percentile Q1 pathway, assuming that 35 canisters fail due to piping (i.e., failure of every canister at risk) would imply peak and million-year release rates of approximately 88 and 5 μSv/yr. This calculated peak release rate implies approximately simultaneous failure, but is unrealistic. Instead, canister failure times would be spread out over the million-year period, because failure time is inversely proportional to the pipe flow rate. Accordingly, the corresponding peak from the ensemble of failed packages is likely to be more like the combined peak from a few canisters rather than all 35 canisters.

We conclude that corrosion failures due to piping could yield releases that are comparable in magnitude to regulatory limits, but it appears difficult to develop a scenario based on piping that generates release rates that are much larger than the regulatory limit. Clearly, the largest consequences require that small pipes through the buffer and contacting the canister would be likely at the extreme end of the hydraulic conditions compatible with the natural system. It is not at all clear that this type of piping would be likely even at such high flow rates.

3. The Consultants' overall assessment

3.1. Motivation of the assessment

SSM concluded from the initial phase of SSM's review of SR-Site that SKB's reporting is sufficiently comprehensive and of sufficient quality to justify a continuation of SSM's review to the main review phase. During the main review phase, SSM developed technical review assignments considering one or several specific issues or areas that SSM deems to require detailed assessment. SSM intends this technical review assignment to (i) consider how the entity Qeq is calculated, (ii) assess if the results and cases SKB has chosen are relevant as input to the calculations of copper corrosion and radionuclide transport, and (iii) assess the relevance of the implementation of the Qeq concept for copper corrosion calculations.

SKB uses the Qeq concept in the context of near-field transport of dissolved species. In our opinion, the Qeq parameter is so intimately linked with near-field transport that assessment of the Qeq parameter as essentially the same as assessing the SKB near-field transport approach, at least with respect to the interaction of flow and diffusive transport. Therefore, we addressed the technical review assignment by considering the following tasks: (i) summarizing the near-field transport methodology and identifying risk-significant aspects, (ii) independently testing risk-significant aspects of the model, and (iii) identifying potential weaknesses in the safety case with respect to near-field transport, in particular canister corrosion.

3.2. The Consultants' assessment

We broke our assessment into three general categories: (i) review of the Qeq documentation, (ii) independent confirmation of corrosion conclusions, and (iii) independent assessment of radionuclide release conclusions.

3.2.1. Assessment of the Qeq documentation

The overall Qeq approach is inherently a network model for steady linear diffusion, with the Qeq parameter consisting of a diffusion coefficient and a geometric factor describing cross-sectional area and diffusion distance. Network models are attractive for probabilistic calculations because they are very fast to evaluate. SKB developed a set of geometric factors to describe diffusion legs for different physical configurations, such as diffusion in a cylinder, radially diverging and converging flow, exchange between a surface and flowing water, and exchange between stagnant and flowing water.

We examined SKB's methodology and description of the methodological limitations, and concluded that (i) the numerical framework is based on widely applied methodology and (ii) reasonable numerical approximations are used to describe the individual diffusion legs. We also compared the use of the Qeq approach across cited documents considering canister corrosion and radionuclide

release, and concluded that (i) consistent methodology is used in both applications, and (ii) consistent parameters are used in both applications.

The Qeq approach implies that diffusive transport is essentially in equilibrium with the endpoint concentrations, or is approximately in a steady state mode. We concluded that this approach is reasonable for corrosion calculations and release calculations of nonsorbing radionuclides. SKB indicates that a transient approach is necessary to model highly retarded radionuclides, but we were unable to identify the calculational procedure that SKB uses for such transient calculations. We note that a steady state approach may be adequate for highly retarded radionuclides even when waste form degradation changes over even longer time scales.

The methodology used to calculate radionuclide transport through the near field appears to be inconsistently described in TR-10-66 (Appendix G.2). The overall approach implies that the pathways should be calculated as branching pathways, which is consistent with associated figures describing the Q1, Q2, and Q3 pathways. In contrast, the description of equivalent resistances for each pathway implies that the pathways are calculated in parallel. If the pathways were calculated in parallel, the same physical location (i.e., at each branch point) would have different concentrations in the different pathways. The total calculated release for parallel pathways would be a factor of 1 to 3 times larger than total calculated release for branching pathways. We suspect that the description of equivalent resistances may not accurately describe the actual approach in COMP23. Even if the error occurs in COMP23, we conclude that the potential error is too small to significantly affect safety-related conclusions.

3.2.2. Assessment of corrosion calculations

We consider the corrosion calculations to be the dominant risk-significant aspect of the Qeq approach because of the very low number of failed canisters resulting from nominal conditions. Accordingly, we focussed our assessment on corrosion.

We relied strongly on independent 2D and 3D numerical modelling to assess SKB results. The independent model was in general agreement with SKB calculations for stagnant conditions within the deposition hole. The model results suggest that higher corrosion rates would occur if hydraulic conditions supported flow converging to the deposition hole. SKB considered convergent flow due to a spalled zone; we also note that a connected pipe inside the deposition hole would have a similar effect. Nevertheless, we conclude that it is extremely unlikely that breakthrough of the copper shell will occur within one million years due to sulphide corrosion if conditions limit transport to diffusion within the deposition hole. This condition would require a combination of (i) time-averaged background sulphide concentrations experienced at the deposition hole during the performance period larger than have been observed at the site to date, (ii) convergent flow to the deposition hole, and (ii) site conditions supporting significant flow to the deposition hole.

We considered the SKB hypothetical scenario of a partially eroded buffer, in which advection increases corrosion rates. It is not clear that the implied large amount of bentonite removal is physically reasonable, and the sizes of the void and exposed copper surface area are difficult to justify. We developed an alternative conceptual model of a worst-case advection scenario, consisting of pipes through the bentonite buffer and contacting the copper for extended durations. Pipes have been created

during laboratory bentonite wetting experiments, but it is not clear that conditions conducive to initiating and maintaining pipes will occur in the field.

Assuming that the pipes are able to persist indefinitely in hydraulic equilibrium with the surrounding fracture system, we established representative sizes and flow rates of pipes in a buffer consistent with flows in a site-scale discrete-fracture realization. Making reasonable assumptions about the hydraulic and geochemical conditions, we estimate that perhaps 0.5 percent of the deposition holes might result in a breached copper shell in less than one million years if the pipes were likely to form.

3.2.3. Assessment of release calculations

Our assessment of radionuclide release was primarily limited to checking consistency with respect to model concepts, inputs, and results. Other than the potential implementation inconsistencies with respect to (i) transient calculations of highly sorbing radionuclides and (ii) parallel/series calculations of resistance, the model generally provided consistent results at the level we examined.

We also considered the consequences of the pipe model with respect to transport, using SKB model results for analogous conditions to estimate release rates. We concluded that corrosion failure leading to radionuclide releases may yield dose consequences close to the regulatory limit, assuming that the pipes easily formed at the high extremes of the flow range. We did not identify conditions that would greatly exceed the regulatory limits.

3.2.4. Overall assessment of the Qeq approach

We consider the Qeq approach implemented by SKB to be a reasonable and practical numerical method, widely applied across a variety of branches of mathematical physics, for approaching the transport of corrodants and radionuclides within the near field. The methods for calculating resistances are based on analytical approaches. Our independent calculations using detailed numerical models provided results consistent with the Qeq approach.

The Qeq approach is most accurate for nonsorbing or weakly sorbing dissolved species, which (i) describes the species of interest for corrosion and (ii) typically provide the largest contributions to dose. Therefore, we conclude that the method performs best on the most risk-significant dissolved constituents. SKB inconsistently describes transport assumptions in the release model; we estimate that an incorrect implementation would overestimate release rates by up to a factor of 3.

Implementation of the Qeq method depends on the conceptual model for the system. Constraints on copper overpack corrosion include (i) flow in the surrounding fracture system, (ii) buffer diffusion, (iii) aspects of the system augmenting flow convergence to the deposition hole, and (iv) advection (or lack thereof) within the deposition hole. The same constraints operate for release, with additional constraints imposed when the penetration area through the canister is small. One of these constraints is typically limiting, thus most risk significant. We consider the Qeq approach well suited for identifying risk-significant constraints.

We consider corrosion failure calculations to be risk-significant compared to radionuclide transport calculations for this site, because it is unlikely that a canister

will fail under the nominal scenario. Our independent calculations for the nominal scenario are consistent with SKB calculations. We developed an alternative conceptual model for estimating worst-case corrosion failure rates, inspired by piping observed in laboratory experiments of bentonite rewetting. The volume of pipes consistent with modelled hydraulic conditions in the fracture system would be at least four orders of magnitude smaller than the void space SKB assumes for a partially eroded buffer, thus the surrounding fracture system would need to convey much less eroded bentonite away from the deposition hole. Assuming that pipes that contact the canisters would be expected to form for the deposition holes with highest flow rates (which we consider a big assumption), we estimate that on the order of 0.5 percent of the canisters might fail within one million years. Applying comparable SKB release calculations to this worst-case scenario, we estimate that expected doses might be comparable to the regulatory limit.

4. References

Bockgård N, 2010. Groundwater flow modelling of an abandoned partially open repository. SKB R-10-41, Svensk Kärnbränslehantering AB.

Joyce S, Simpson T, Hartley L, Applegate D, Hoek J Jackson P, Swan D, Marsic N, Follin S, 2010. Groundwater flow modelling of periods with temperate climate conditions – Forsmark. SKB R-09-20, Svensk Kärnbränslehantering AB.

Neretnieks I, Liu L, Moreno L, 2010. Mass transfer between waste canister and water seeping in rock fractures. Revisiting the Q-equivalent model. SKB TR-10-42, Svensk Kärnbränslehantering AB.

Sandén T, Börgesson L, 2010. Early effects of water inflow into a deposition hole. SKB R-10-70, Svensk Kärnbränslehantering AB.

Selroos J-O, 2010. SR-Site groundwater flow modelling methodology, setup, and results. SKB R-09-22, Svensk Kärnbränslehantering AB.

SKB, 2011. Long-term safety for the final repository at Forsmark: Main report of the SR-Site project. SKB TR-11-01, Svensk Kärnbränslehantering AB.

SKB, 2010. Buffer, backfill and closure process report for the safety assessment SR-Site. SKB TR-10-47, Svensk Kärnbränslehantering AB.

SKB, 2010. Radionuclide transport report for the safety assessment SR-Site. SKB TR-10-50, Svensk Kärnbränslehantering AB.

SKB, 2010. Data report for the safety assessment SR-Site. SKB TR-10-52, Svensk Kärnbränslehantering AB.

SKB, 2010. Corrosion calculations report for the safety assessment SR-Site. SKB TR-10-66, Svensk Kärnbränslehantering AB.

SSM2011-2426-130. Excel file “hydrogeological_base_case_r0_velocity.xls”. SKBdoc id 1396328 ver 1.0, Svensk Kärnbränslehantering AB.

Vidstrand P, Follin S, Zugec N, 2010. Groundwater flow modelling of periods with periglacial and glacial climate conditions – Forsmark. SKB R-09-21, Svensk Kärnbränslehantering AB.

APPENDIX 1

Coverage of SKB reports

Table 1-1: SKB reports reviewed during the assessment

Reviewed report	Reviewed sections	Comments
R-09-20, Groundwater flow modelling of periods with temperate climate conditions – Forsmark	Entire report	Overview only
R-09-21, SR-Site groundwater flow modelling methodology, setup, and results	Entire report	Overview only
R-09-22, Groundwater flow modelling of periods with periglacial and glacial climate conditions – Forsmark	Entire report	Overview only
R-10-41, Groundwater flow modelling of an abandoned partially open repository	Chapter 4	Overview only
R-10-70, Early effects of water inflow into a deposition hole	Entire report	Overview only
TR-10-42, Mass transfer between waste canister and water seeping in rock fractures. Revisiting the Q-equivalent model	Entire report	Focused assessment
TR-10-47, Buffer, backfill and closure process report for the safety assessment SR-Site	Section 3.3.4	Overview only
TR-10-50, Radionuclide transport report for the safety assessment SR-Site	Entire report	Focused assessment
TR-10-52, Data report for the safety assessment SR-Site	Chapter 6	Overview only
TR-10-66, Corrosion calculations report for the safety assessment SR-Site	Chapters 4, 5.3; App. 1	Focused assessment
TR-11-01, Long-term safety for the final repository at Forsmark: Main report of the SR-Site project	Chapters 8.3, 10.3-10.5, 12, 13	Context assessment

2013:36

The Swedish Radiation Safety Authority has a comprehensive responsibility to ensure that society is safe from the effects of radiation. The Authority works to achieve radiation safety in a number of areas: nuclear power, medical care as well as commercial products and services. The Authority also works to achieve protection from natural radiation and to increase the level of radiation safety internationally.

The Swedish Radiation Safety Authority works proactively and preventively to protect people and the environment from the harmful effects of radiation, now and in the future. The Authority issues regulations and supervises compliance, while also supporting research, providing training and information, and issuing advice. Often, activities involving radiation require licences issued by the Authority. The Swedish Radiation Safety Authority maintains emergency preparedness around the clock with the aim of limiting the aftermath of radiation accidents and the unintentional spreading of radioactive substances. The Authority participates in international co-operation in order to promote radiation safety and finances projects aiming to raise the level of radiation safety in certain Eastern European countries.

The Authority reports to the Ministry of the Environment and has around 270 employees with competencies in the fields of engineering, natural and behavioural sciences, law, economics and communications. We have received quality, environmental and working environment certification.

Strålsäkerhetsmyndigheten
Swedish Radiation Safety Authority

SE-171 16 Stockholm
Solna strandväg 96

Tel: +46 8 799 40 00
Fax: +46 8 799 40 10

E-mail: registrator@ssm.se
Web: stralsakerhetsmyndigheten.se